THE JOURNAL OF CELL BIOLOGY

Interaction between autism-linked MDGAs and neuroligins suppresses inhibitory synapse development

Katherine L. Pettem, Daisaku Yokomaku, Hideto Takahashi, Yuan Ge, and Ann Marie Craig

Brain Research Centre and Department of Psychiatry, University of British Columbia, Vancouver, British Columbia V6T 2B5, Canada

Rare variants in *MDGAs* (MAM domain–containing glycosylphosphatidylinositol anchors), including multiple protein-truncating deletions, are linked to autism and schizophrenia, but the function of these genes is poorly understood. Here, we show that MDGA1 and MDGA2 bound to neuroligin-2 inhibitory synapse–organizing protein, also implicated in neurodevelopmental disorders. MDGA1 inhibited the synapse-promoting activity of neuroligin-2, without altering neuroligin-2 surface trafficking, by inhibiting interaction of neuroligin-2 with neurexin. MDGA binding and suppression of synaptogenic activity was selective for neuroligin-2 and not neuroligin-1 excitatory synapse organizer. Overexpression of MDGA1 in cultured rat hippocampal neurons reduced inhibitory synapse density without altering excitatory synapse density. Furthermore, RNAi-mediated knockdown of MDGA1 selectively increased inhibitory but not excitatory synapse density. These results identify MDGA1 as one of few identified negative regulators of synapse development with a unique selectivity for inhibitory synapses. These results also place *MDGAs* in the neurexin–neuroligin synaptic pathway implicated in neurodevelopmental disorders and support the idea that an imbalance between inhibitory and excitatory synapses may contribute to these disorders.

Introduction

Recent genetic studies implicated a number of synaptic cell adhesion molecules and their intracellular partners in both autism spectrum disorders (ASDs) and schizophrenia (Betancur et al., 2009; Bourgeron, 2009). Among these, *NRXN1* encoding neurexin-1 is one of the genes most strongly linked to nonsyndromic ASDs through copy number variants and sequence alterations (Szatmari et al., 2007; Südhof, 2008; Sanders et al., 2011). Function-altering variants in neurexins *NRXN2* (Gauthier et al., 2011) and *NRXN3* (Vaags et al., 2012) and trans-synaptic binding partner neuroligins *NLGN1–4* (Südhof, 2008; Glessner et al., 2009; Sun et al., 2011) are also linked to ASDs and schizophrenia. The idea that a rare variant in one of these individual genes may confer substantial risk for such psychiatric disorders is supported by animal models. Mice with mutations in *NLGN3* or *NLGN4* mimicking disease variants exhibit selective behavioral deficits in social interaction (Tabuchi et al., 2007; Jamain et al., 2008).

Neuroligins and neurexins function as synapse-organizing proteins, mediating cell adhesion and recruiting components to developing synapses (Südhof, 2008; Siddiqui and Craig, 2011; Krueger et al., 2012). Neuroligin function is important for fundamental aspects of synapse development, supported by the perinatal lethal phenotype of mice lacking neuroligin-1, -2, and -3 (Varoqueaux et al., 2006). Neuroligin-1 localizes selectively to excitatory postsynaptic sites (Song et al., 1999) and overexpression enhances excitatory synapse development (Chih et al., 2005). Mice lacking neuroligin-1 exhibit selective deficits in NMDA receptor-mediated glutamatergic transmission (Chubykin et al., 2007), and additional knockdown of neuroligin-3 and other neurexin partners such as LRRTMs suggests that neuroligin-1 cooperatively contributes to AMPA receptor-mediated transmission (Soler-Llavina et al., 2011). Neuroligin-2 localizes selectively to inhibitory synapses (Graf et al., 2004; Varoqueaux et al., 2004), interacts with collybistin inhibitory postsynaptic protein (Poulopoulos et al., 2009), and mice lacking neuroligin-2 exhibit deficits in postsynaptic composition

K.L. Pettem and D. Yokomaku contributed equally to this paper

Correspondence to Ann Marie Craig: acraig@mail.ubc.ca

Abbreviations used in this paper: ASD, autism spectrum disorder; Fc, fragment crystallizable; FNIII, fibronectin type III; GPI, glycosylphosphatidylinositol; MAM, memprin, A5 protein, receptor protein tyrosine phosphatase mu; MDGA, MAM domain–containing glycosylphosphatidylinositol anchor.

The Rockefeller University Press $30.00
J. Cell Biol. Vol. 200 No. 3 321–336
www.jcb.org/cgi/doi/10.1083/jcb.201206028

and function at subsets of inhibitory synapses (Chubykin et al., 2007; Gibson et al., 2009; Poulopoulos et al., 2009).

MDGA1 (MAM domain–containing glycosylphosphatidylinositol anchor 1) and *MDGA2* were also recently implicated in ASDs and schizophrenia. Intronic single nucleotide polymorphisms in *MDGA1* were linked to schizophrenia in multiple independent studies (Kähler et al., 2008; Li et al., 2011), and protein-truncating variants were found in *MDGA2* in 10 unrelated ASD cases, a statistically significant association (Bucan et al., 2009). MDGAs are strongly expressed in basilar pons, and MDGA1 also shows higher expression than MDGA2 in superficial cortical layers, hippocampus, amygdala, thalamus, olfactory bulb, and cerebellum (Litwack et al., 2004; Lein et al., 2007). Although RNAi knockdown suggested a role for MDGA1 in developing cortical neuron migration (Takeuchi and O'Leary, 2006), genetic deletion revealed only a transient role with normal cortical lamination by 2 wks postnatal in the absence of MDGA1 (Ishikawa et al., 2011). MDGAs contain six extracellular immunoglobulin-like (Ig) domains, a fibronectin type III-like (FNIII) domain, a memprin, A5 protein, receptor protein tyrosine phosphatase mu (MAM) domain, and a glycosylphosphatidylinositol (GPI) anchor, suggesting they participate in protein interactions. Binding of MDGA1 ectodomain to brain sections has been observed (Fujimura et al., 2006), but binding partners have not yet been reported. Several other genes with Ig and/or FNIII domains and linked to autism including *CADM1* (Zhiling et al., 2008), *IL1RAPL1* (Piton et al., 2008), *LRFN5* (de Bruijn et al., 2010), and *PTPRD* (Pinto et al., 2010) function in synaptic adhesion and synapse organization (Biederer et al., 2002; Mah et al., 2010; Valnegri et al., 2011; Yoshida et al., 2011; Takahashi et al., 2012). Thus, we hypothesized that *MDGA*s might function in regulating synapse development. Here, we report that MDGAs bind to neuroligin-2, and through overexpression and knockdown experiments show that MDGA1 is a negative regulator of neuroligin-2 synaptogenic function. These results reveal MDGA1 as a suppressor of inhibitory synapse development and link MDGAs to the synaptic pathway implicated in ASDs and schizophrenia.

Results

MDGA1 and MDGA2 bind neuroligin-2

Based on the brain-specific expression of MDGAs (Litwack et al., 2004), the presence of cell adhesion domains, and links to ASDs and schizophrenia (Kähler et al., 2008; Bucan et al., 2009; Li et al., 2011), we hypothesized that MDGAs may play a role in synaptic development. Initial tests in neuron–fibroblast co-culture hemi-synapse induction assays, as detailed further below, led us to suspect that MDGAs might interact with neuroligins. Because MDGAs are GPI anchored, such interaction would have to occur via extracellular domains. A common method to demonstrate interaction of protein extracellular domains such as for neurexin–neuroligin is to incubate cultured cells expressing neurexin with soluble recombinant neuroligin ectodomain or vice versa (Boucard et al., 2005; Chih et al., 2006; Siddiqui et al., 2010). Thus, to test for binding between MDGAs and neuroligins, we generated soluble ectodomain fusion proteins of neuroligin-1 and neuroligin-2 with the human Fc (fragment crystallizable) antibody region (Nlg1-Fc and Nlg2-Fc) and assayed binding to COS7 cells expressing HA-tagged MDGAs. Binding of Nlg2-Fc was observed to cells expressing HA-MDGA1 or HA-MDGA2, similar to cells expressing HA-neurexin1β, whereas no binding was observed to untransfected cells or cells expressing nonspecific control protein HA-CD4 (Fig. 1 A). Binding assays over a range of concentrations revealed saturated binding of Nlg2-Fc to both HA-MDGA1 and HA-MDGA2 (Fig. 1 B). By Scatchard analysis, we found an apparent dissociation constant (K_d) of 7.3 ± 1.0 nM for Nlg2-Fc binding to HA-MDGA1 and 45.9 ± 11.9 nM for Nlg2-Fc binding to HA-MDGA2. In the same assays, the apparent K_d for Nlg2-Fc binding to HA-neurexin1β was 8.4 ± 1.1 nM. These binding affinities are in the nanomolar range typically observed for physiologically significant ligand–receptor interactions. Based on the lower binding affinity of Nlg2-Fc as well as the much lower expression in the brain (Lein et al., 2007) for MDGA2 compared with MDGA1, we focused on MDGA1 for the remainder of our analysis.

We next tested binding of neuroligin-1 to MDGA1 in the same way, testing the most common neuroligin-1 variant with the insert at the B splice site (+B). There appeared to be Nlg1-Fc signal associated with HA-MDGA1–expressing cells when incubated with very high concentrations of Nlg1-Fc, but using concentrations as high as 800 nM we were unable to observe saturated binding (Fig. 1 D). The observed signal may represent weak interaction. Assaying binding at 200 nM, a concentration sufficient to readily detect binding of Nlg1-Fc to HA-neurexin1β and of Nlg2-Fc to MDGAs, the binding signal of Nlg1-Fc was not significantly higher for HA-MDGA1 than for the nonspecific control HA-CD4 (Fig. 1, C and D). Thus, MDGA1 showed little interaction with neuroligin-1(+B), in contrast to high affinity interaction with neuroligin-2.

Assays for binding of neurexin-1β-Fc to cells expressing HA-MDGA1 showed no signal compared with robust binding to cells expressing HA–neuroligin-2 (not depicted). Thus, MDGA1 does not directly interact with the neuroligin-2 trans-synaptic partner, neurexin.

MDGA1 has six Ig domains, a FNIII domain, and a MAM domain (Fig. 2 A). To determine the domains responsible for binding to neuroligin-2, various deletion constructs were generated to eliminate each of the first three Ig repeats individually (ΔIg1, ΔIg2, ΔIg3), the first three Ig repeats together (ΔIg1-3), the last three Ig repeats together (ΔIg4-6), the FNIII domain (ΔFNIII), the MAM domain (ΔMAM), and all domains except the first three Ig domains (Ig1-3 only). These constructs were transfected into COS7 cells and assayed for binding of Nlg2-Fc (Fig. 2, B and C). Binding was abolished when any one of the first three Ig repeats were removed, whereas binding was preserved with only the first three Ig repeats present, indicating that the Ig repeats 1–3 are necessary and sufficient for MDGA1 binding to neuroligin-2.

MDGA1 inhibits induction of presynaptic differentiation by neuroligin-2

To functionally characterize the interaction between MDGA1 and neuroligin-2, we used the neuron–fibroblast co-culture assay.

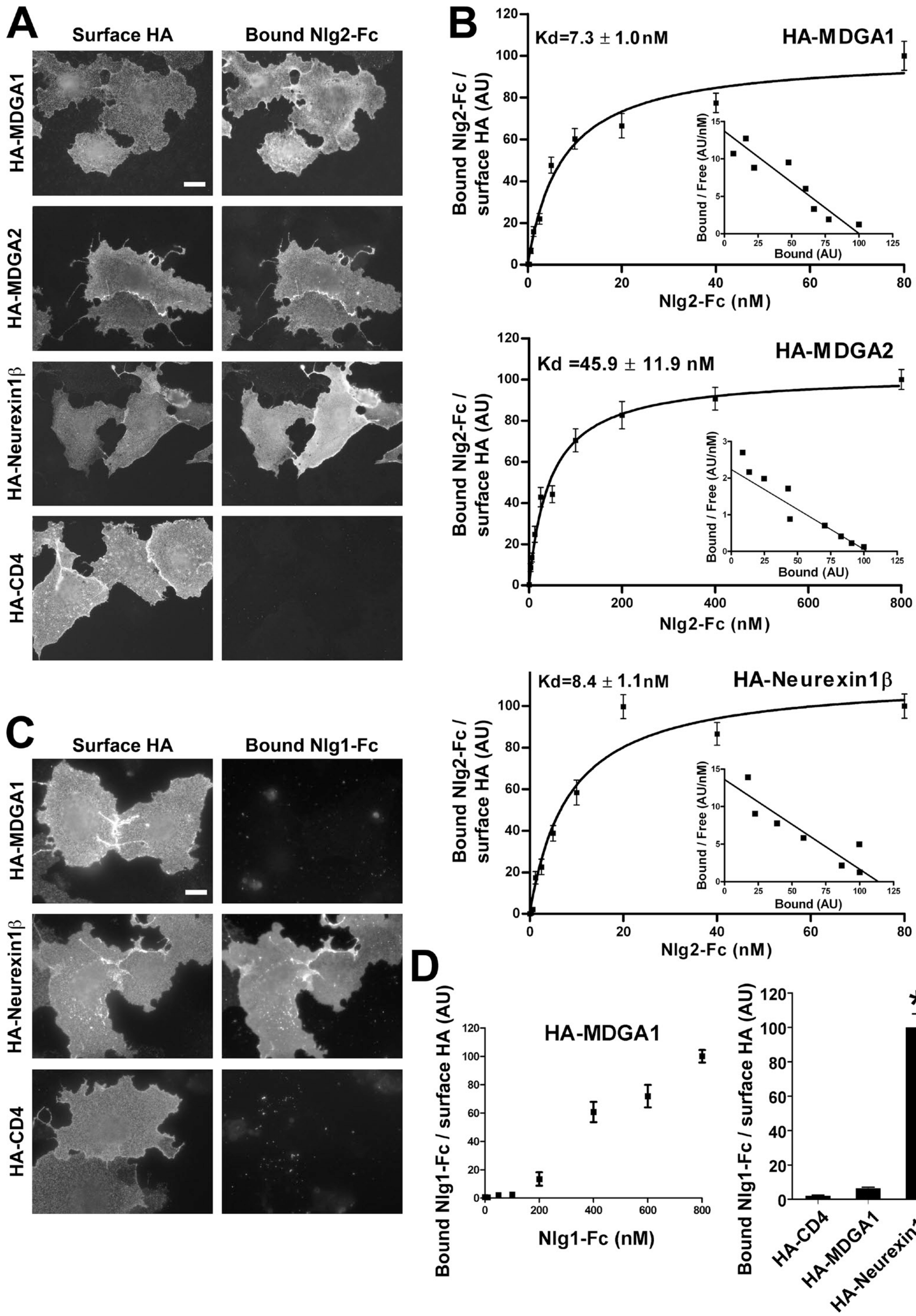

Figure 1. **MDGAs bind to neuroligin-2 via ectodomain interactions.** (A) Soluble neuroligin-2–Fc fusion protein (Nlg2-Fc) bound to COS7 cells expressing HA-MDGA1, HA-MDGA2, or HA-neurexin1β, but not HA-CD4, on the cell surface. (B) By Scatchard analysis, binding affinity of Nlg2-Fc to HA-MDGA1, HA-MDGA2, and HA-neurexin1β was characterized by an estimated dissociation constant (K_d) of 7.3, 45.9, and 8.4 nM, respectively (n = 20 cells each data point). (C) Neuroligin-1–Fc fusion protein (Nlg1-Fc) bound clearly to COS7 cells expressing HA-neurexin1β, but not HA-MDGA1 or HA-CD4. (D) Incubation of Nlg1-Fc with COS7 cells expressing HA-MDGA1 did not yield saturable binding at concentrations up to 800 nM (n = 10 cells each). At a concentration of 200 nM Nlg1-Fc, quantitation of bound Nlg1-Fc divided by surface HA and normalized to the value for HA-neurexin1β revealed little or no Nlg1-Fc binding to COS7 cells expressing HA-MDGA1. ANOVA, $P < 0.0001$, n = 30 cells each; *, $P < 0.001$ compared with HA-CD4 by post-hoc Bonferroni test. Data are mean ± SEM. Bars, 20 µm.

Neuroligin-2 expressed in COS7 cells induces presynaptic differentiation in contacting axons; by binding neurexins on axons, neuroligin-2 locally clusters presynaptic proteins in the absence of postsynaptic proteins or dendrites (Scheiffele et al., 2000; Dean et al., 2003; Craig et al., 2006). Here, we imaged clustering of the presynaptic protein synapsin in axons contacting COS7

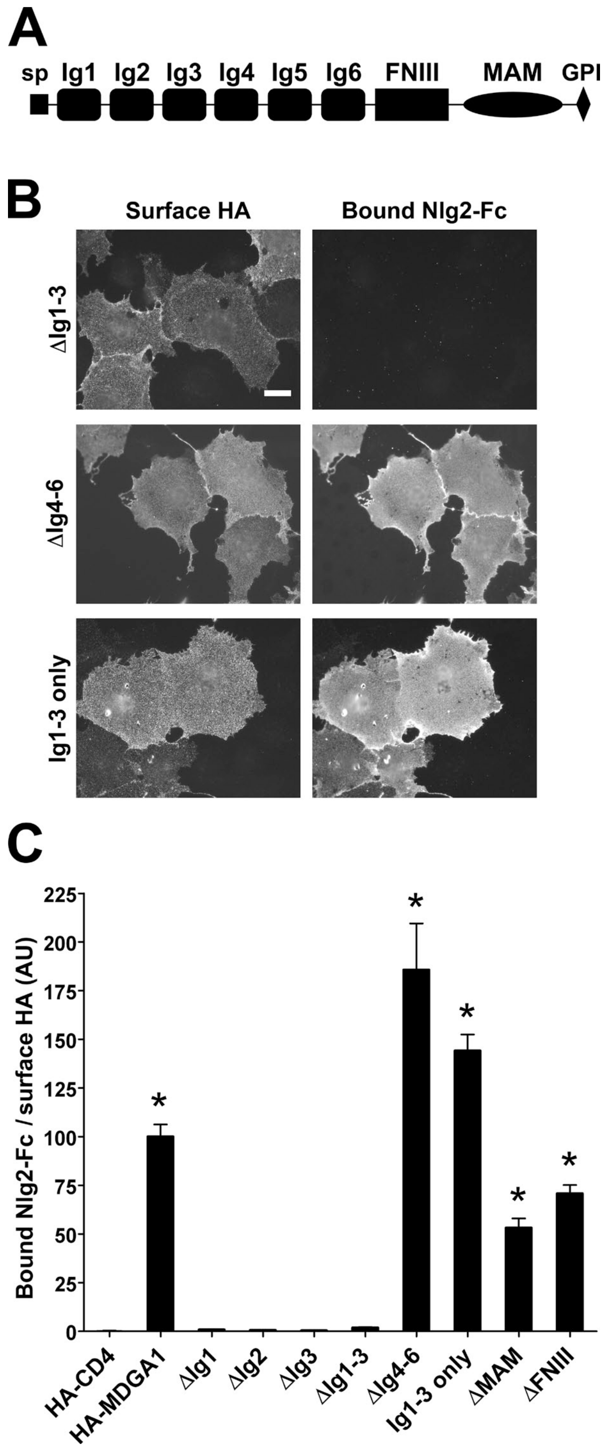

Figure 2. **MDGA1 Ig1-3 domains bind neuroligin-2.** (A) Domain structure of MDGA1. MDGA1 is composed of an N-terminal signal peptide (sp), six immunoglobulin domains (Ig), a fibronectin type III domain (FNIII), a meprin, A5 protein, receptor tyrosine phosphatase mu (MAM) domain, and a C-terminal GPI anchor. (B) Representative images from binding assays of Nlg2-Fc to HA-MDGA1 mutants. Nlg2-Fc bound to HA-MDGA1 lacking the last three Ig domains (ΔIg4-6), but not HA-MDGA1 lacking the first three Ig domains (ΔIg1-3). Note that the first three Ig domains of MDGA1 plus the GPI anchor (Ig1-3 only) were sufficient for Nlg2-Fc binding. (C) Quantitation of Nlg2-Fc bound to HA-MDGA1 mutants, divided by surface HA and normalized to the value for HA-MDGA1. The membrane-associated Ig1-3 domains were necessary and sufficient for binding of Nlg2-Fc. ANOVA, $P < 0.0001$, $n \geq 45$ cells each; *, $P < 0.001$ compared with HA-CD4 by post-hoc Bonferroni test. Data are mean ± SEM. Bar, 20 µm.

cells transfected for CFP–neuroligin-2 and HA-MDGA1 (where different COS7 cells express different ratios of the transfected constructs). Synapsin clustering in axons contacting COS7 cells coexpressing HA-MDGA1 with CFP–neuroligin-2 appeared greatly diminished compared with COS7 cells expressing CFP–neuroligin-2 alone (Fig. 3 A). Quantitatively, coexpression of HA-MDGA1 with CFP–neuroligin-2 significantly reduced synapsin clustering in axons contacting transfected COS7 cells compared with coexpression of control protein HA-CD4 (Fig. 3, B and C). HA-MDGA1 also reduced the total level of CFP–neuroligin-2 (Fig. 3 D). When analysis was limited to cells with equivalent levels of CFP–neuroligin-2, HA-MDGA1 in comparison to HA-CD4 control still suppressed the presynaptic inducing activity of neuroligin-2 (Fig. 3 E). We performed another co-culture experiment to assess specifically inhibitory presynaptic differentiation and axon contact. Coexpression of HA-MDGA1 or HA-CD4 control resulted in equivalent contact area of tau-positive axons with COS7 cells expressing CFP–neuroligin-2 (Fig. 3 F and Fig. S1 A). However, coexpression of HA-MDGA1 with CFP–neuroligin-2 reduced clustering of the inhibitory presynaptic vesicular GABA transporter VGAT in axons contacting the transfected COS7 cells compared with coexpression of HA-CD4, both for the entire dataset and for the subset selected for equivalent CFP–neuroligin-2 levels (Fig. S1). Thus, the major mechanism by which MDGA1 suppresses inhibitory synapse development appears to be independent of the extent of axon contact and level of neuroligin-2, at least in co-culture. In a similar co-culture assay, coexpression of HA-MDGA1 or HA-CD4 control with CFP–neuroligin-1(+B) resulted in equivalent synapsin clustering and CFP–neuroligin-1 level (Fig. 3, B and H; and unpublished data). Thus, MDGA1 selectively inhibits the synaptogenic activity of neuroligin-2.

To determine which domains of MDGA1 are important for the inhibition of neuroligin-2 synaptogenic activity, we performed similar co-culture experiments coexpressing CFP–neuroligin-2 with various HA-MDGA1 deletion constructs. Deletion of the first three Ig domains together or individually from MDGA1 restored full presynaptic induction activity for neuroligin-2 (Fig. 4, A and C), whereas coexpressing the Ig1-3 only construct was sufficient to suppress neuroligin-2 to the same extent as full-length MDGA1 (Fig. 4, B and C). The last three Ig domains, FNIII domain, and MAM domain were not required for MDGA1 to suppress neuroligin-2 activity in co-culture (Fig. 4 C). These results indicate that the Ig1-3 domains, which are necessary and sufficient for binding to neuroligin-2, are also necessary and sufficient to suppress the synapse-promoting activity of neuroligin-2 in co-culture.

MDGA1 inhibits binding of neurexin to neuroligin-2

Because neuroligins induce presynaptic differentiation by binding to neurexins on axons (Scheiffele et al., 2000; Dean et al., 2003), we hypothesized that perhaps MDGA1 blocks the interaction of neuroligin-2 with neurexins. To test this idea, we used another variation of the cell-based protein-binding assay. COS7 cells were cotransfected for CFP–neuroligin-2 and HA-MDGA1, then incubated with soluble neurexin1β ectodomain fusion protein (Nrxn1β-Fc). In cells expressing only CFP–neuroligin-2, strong

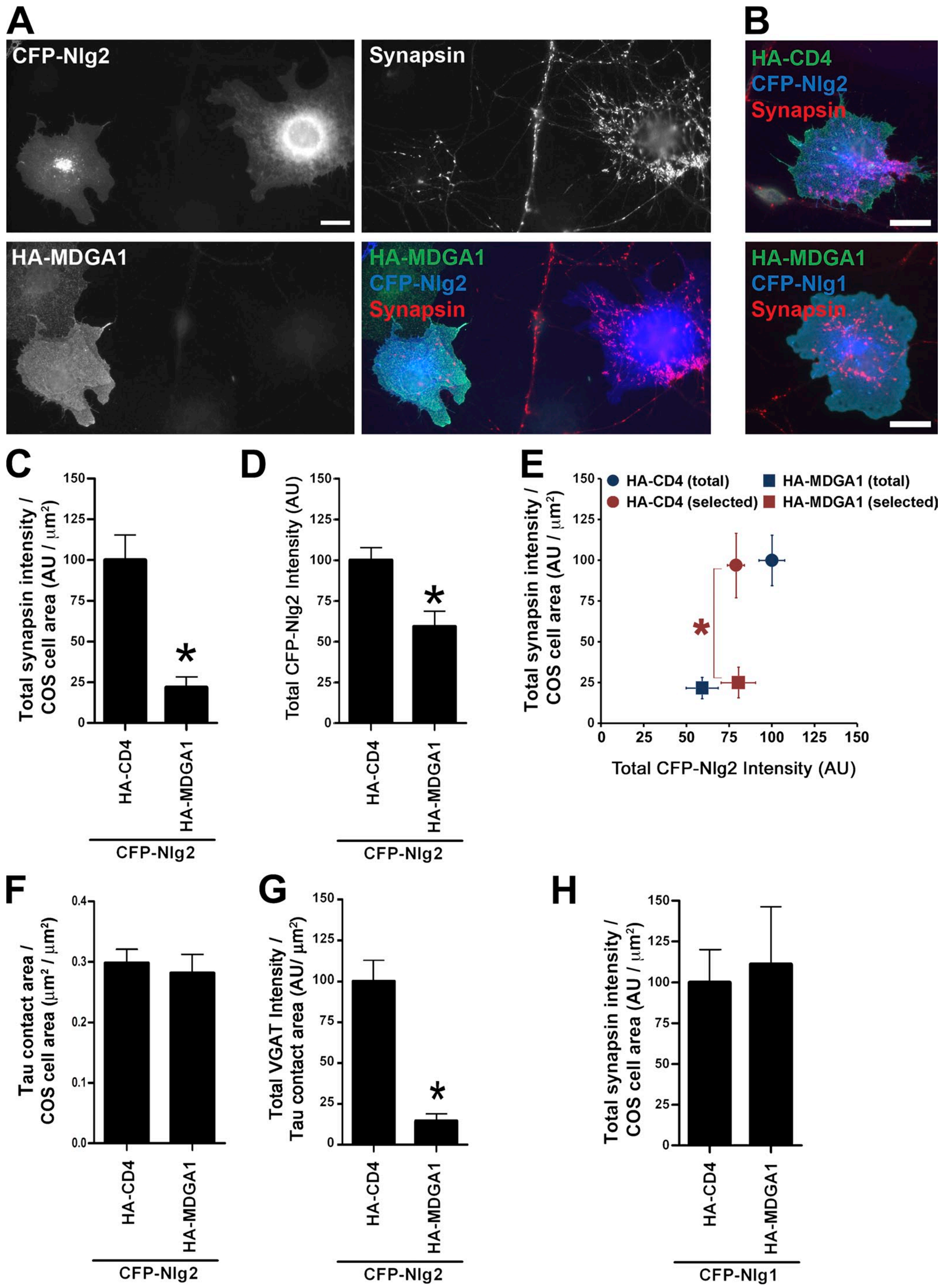

Figure 3. **MDGA1 inhibits the synaptogenic activity of neuroligin-2.** (A) COS7 cells were cotransfected with CFP–neuroligin-2 (CFP-Nlg2) and HA-MDGA1, then co-cultured with hippocampal neurons. COS7 cells expressing only CFP-Nlg2 (e.g., COS7 cell on right) induced robust clustering of synapsin in contacting axons, whereas COS7 cells coexpressing HA-MDGA1 with CFP-Nlg2 (e.g., COS7 cell on left) showed diminished synapsin clustering. (B) Robust synapsin clustering was detected in axons contacting COS7 cells coexpressing HA-CD4 with CFP-Nlg2 (top) or coexpressing HA-MDGA1 with CFP–neuroligin-1 (CFP-Nlg1, bottom). (C) Quantitation of total integrated intensity of synapsin immunofluorescence not associated with MAP2 and associated with COS7 cells coexpressing HA-CD4 or HA-MDGA1 with CFP-Nlg2, divided by COS7 cell area and normalized to the value for HA-CD4. *t* test; *, $P < 0.0001$, $n = 20$ cells each. (D) Quantitation of total fluorescent intensity of CFP-Nlg2 on the COS7 cells used for C. *t* test; *, $P < 0.0001$, $n = 20$ cells each. (E) Comparison of total integrated synapsin intensity of selected COS7 cells expressing HA-MDGA1 or HA-CD4 with similar total CFP-Nlg2 expression level ($n = 13$ cells each, red symbols). *t* test; *, $P < 0.0001$. Full datasets from C and D are shown for comparison (blue symbols). (F) Quantitation of tau-positive axon contact area on COS7 cells coexpressing HA-CD4 or HA-MDGA1 with CFP-Nlg2, divided by COS7 cell area. *t* test, $P = 0.67$, $n = 20$ cells each. (G) Quantitation of total integrated intensity of VGAT immunofluorescence not associated with MAP2 and associated with COS7 cells coexpressing HA-CD4 or HA-MDGA1 with CFP-Nlg2, divided by tau-positive axon contact area and normalized to the value for HA-CD4. *t* test; *, $P < 0.0001$, $n = 20$ cells each. (H) Quantitation of total integrated intensity of synapsin immunofluorescence not associated with MAP2 and associated with COS7 cells coexpressing HA-CD4 or HA-MDGA1 with CFP-Nlg1, divided by COS7 cell area and normalized to the value for HA-CD4. *t* test, $P = 0.78$, $n = 20$ cells each. Data are mean ± SEM. Bars, 20 μm.

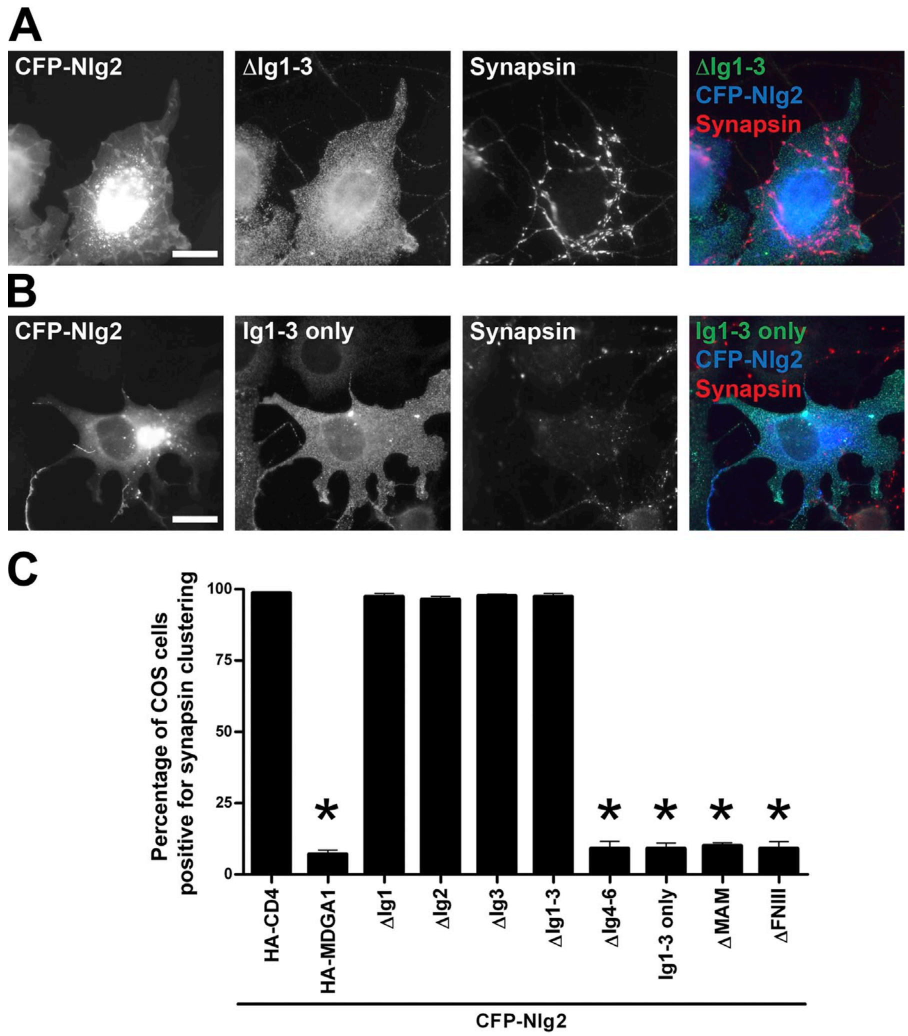

Figure 4. **MDGA1 Ig1-3 domains suppress neuroligin-2 synaptogenic activity.** (A and B) Co-expression of HA-MDGA1 Ig1-3 only (B), but not HA-MDGA1 ΔIg1-3 (A), diminished CFP–neuroligin-2 (CFP-Nlg2)–induced synapsin clustering. (C) Quantitation of the effect of MDGA1 mutants on CFP-Nlg2–induced synapsin clustering in the co-culture assay. Data are expressed as a percentage of COS7 cells coexpressing the indicated construct with CFP-Nlg2 that exhibited synapsin clustering in MAP2-negative contacting neurites. The membrane-anchored Ig1-3 domains of MDGA1 were necessary and sufficient for inhibiting the activity of neuroligin-2 to induce synapsin clustering. ANOVA, $P < 0.0001$, $n \geq 3$ experiments counting ≥100 cells each; *, $P < 0.01$ compared with HA-CD4 by post-hoc Bonferroni test. Data are mean ± SEM. Bars, 20 µm.

binding of Nrxn1β-Fc was observed as expected, but in cells expressing both CFP–neuroligin-2 and HA-MDGA1, binding of Nrxn1β-Fc was markedly reduced (Fig. 5 A). Quantitatively, coexpression of HA-MDGA1 compared with HA-CD4 control significantly reduced binding of Nrxn1β-Fc to cells expressing CFP–neuroligin-2, expressed as Nrxn1β-Fc bound per total CFP–neurolign-2 or per surface CFP–neuroligin-2 (Fig. 5, B and C). In these experiments, as expected from Fig. 3, cells coexpressing MDGA1 compared with CD4 showed a lower average expression level for CFP–neuroligin-2, but when cells with equivalent surface CFP–neuroligin-2 level were compared, a robust effect of MDGA on Nrxn1β-Fc binding was still observed (Fig. 5 D).

As an independent method of assessing the effect of MDGA1 on neurexin–neuroligin interaction, we used a plate-binding ELISA assay with purified recombinant fusion proteins of each of the three ectodomains. An alkaline phosphatase (AP) fusion protein of the ectodomain of neurexin1β, Nrxn1β-AP, was immobilized on plates and incubated with Nlg2-Fc together with either MDGA1-AP or control AP. MDGA1-AP compared with control AP significantly reduced binding of Nlg2-Fc to the immobilized Nrxn1β (Fig. 5 E). Thus, MDGA1 directly reduces interaction of the neuroligin-2 ectodomain with the neurexin1β ectodomain.

MDGA1 does not affect surface trafficking of neuroligin-2

To assess whether MDGA1 alters surface trafficking of neuroligin-2, we used both imaging and surface biotinylation approaches. By the imaging method, cells coexpressing HA-MDGA1 or control HA-CD4 showed equivalent surface trafficking of CFP–neuroligin-2 measured as the intensity ratio of surface anti-GFP antibody signal to total CFP–neuroligin-2 signal (Fig. 6, A and B). By the biochemical method, cells coexpressing YFP-MDGA1 or control YFP-CD4 showed equivalent surface-biotinylated fractions of HA–neuroligin-2 (Fig. 6, C and D). These data indicate that MDGA1 does not interfere with surface trafficking of neuroligin-2, supporting the idea that it inhibits binding of neuroligin-2 to its partner neurexin in some direct way on the cell surface.

Recombinant MDGA1 and neuroligin-2 interact in cis on dendrites

We attempted to determine the subcellular localization of native MDGA1 but were unable to do so due to lack of a suitable antibody. Recombinant YFP-MDGA1 expressed at low level in cultured neurons trafficked to the surface of dendrites and axons (Fig. S2 A). Within dendrites, some clusters of YFP-MDGA1

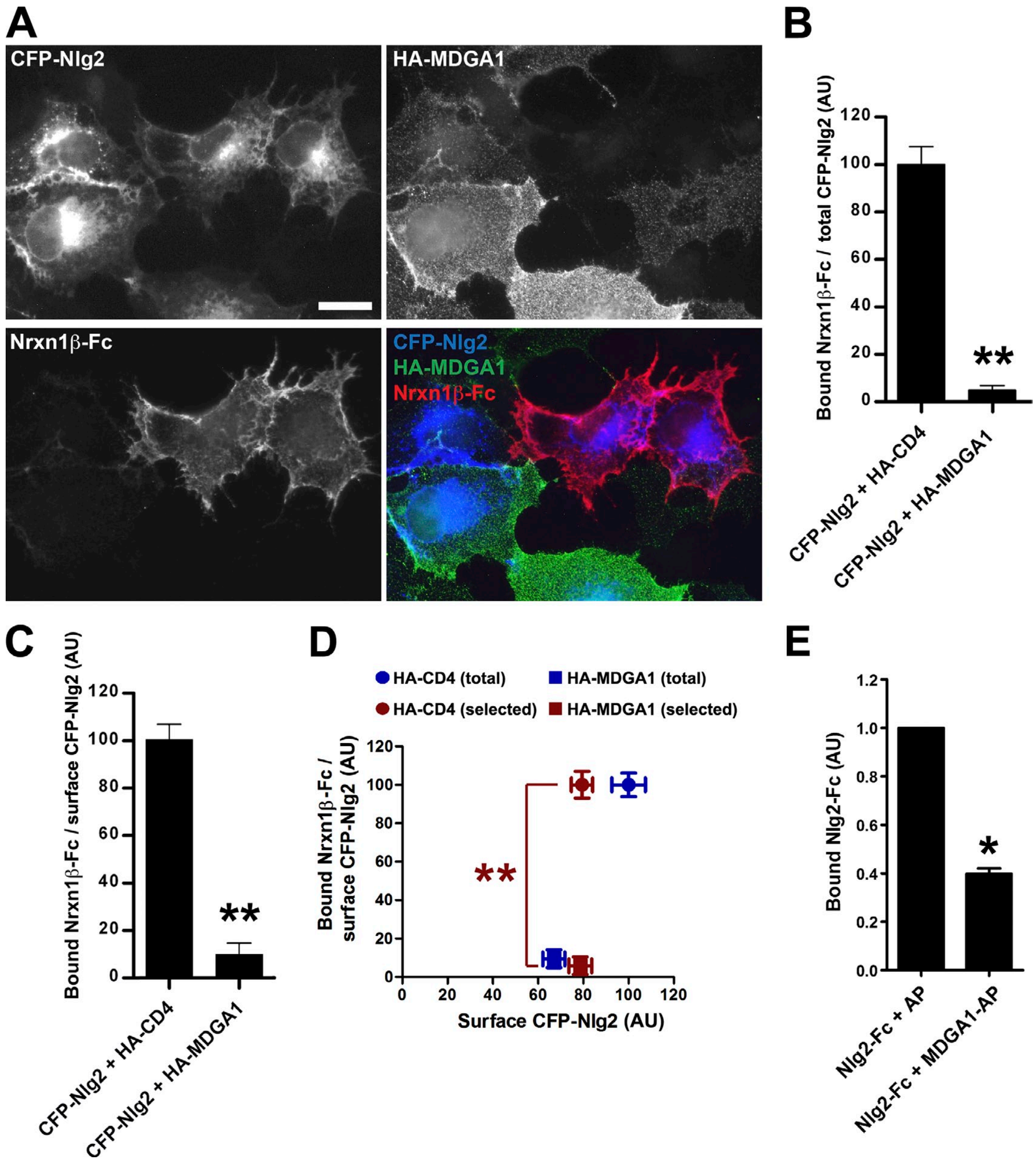

Figure 5. **MDGA1 inhibits the binding of neurexin1β to neuroligin-2.** (A) COS7 cells were transfected with CFP–neuroligin-2 (CFP-Nlg2) and HA-MDGA1. Soluble neurexin1β-Fc fusion protein (Nrxn1β-Fc) bound to cells expressing only CFP-Nlg2 (cells in top right of image), but did not bind to cells coexpressing HA-MDGA1 with CFP-Nlg2 (cells in bottom left of image). (B–D) Quantitation of Nrxn1β-Fc bound to COS7 cells expressing the indicated constructs, divided by total CFP-Nlg2 (B) or by surface CFP-Nlg2 (C and D) and normalized to the value for HA-CD4. HA-MDGA1 compared with HA-CD4 reduced the total and surface levels of CFP-Nlg2, so a subset of cells selected for equal surface expression of CFP-Nlg2 was also compared (red in D; the full dataset is shown for comparison in blue). *t* test; **, $P < 0.0001$, n = 20–30 cells each. (E) Purified neurexin1β-AP (alkaline phosphatase) fusion protein immobilized on plates was incubated with purified Nlg2-Fc together with either MDGA1-AP or AP control. Bound Nlg2-Fc measured by ELISA was reduced in the presence of MDGA1-AP. *t* test; *, $P < 0.005$, n = 3.

were observed colocalizing with gephyrin at inhibitory postsynaptic sites, some with PSD-95 at excitatory postsynaptic sites, and some were extrasynaptic (Fig. S2 B). Thus, it seems likely that MDGA1 may partially concentrate at inhibitory postsynaptic sites but also be distributed elsewhere in neurons.

To assess whether neuroligin-2 and MDGA1 can interact in dendrites, we artificially induced aggregation of HA–neuroligin-2 on the dendrite surface by live-cell incubation with multivalent anti-HA antibody complexes and assessed whether YFP-MDGA1 was recruited. Indeed, YFP-MDGA1, but not control protein YFP-CD4, showed robust co-aggregation with HA–neuroligin-2 at induced nonsynaptic clusters (Fig. 7). Thus, MDGA1 and neuroligin-2 can interact in cis on the dendrite surface.

Overexpression of MDGA1 decreases inhibitory synapse density

Next, we tested the effects of MDGA1 overexpression in cultured hippocampal neurons (DIV 9→DIV 14; Fig. 8, A and B). Overexpression of HA-MDGA1 significantly reduced inhibitory

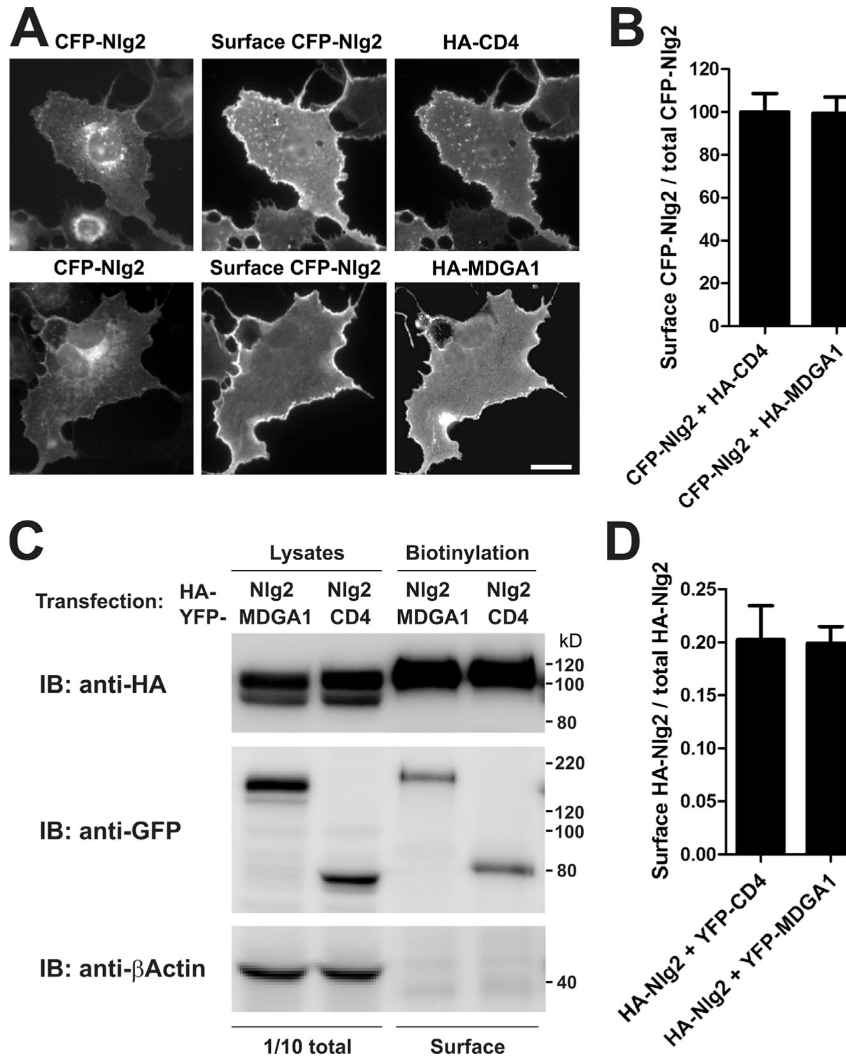

Figure 6. **MDGA1 does not alter surface trafficking of neuroligin-2.** (A) COS7 cells were transfected with CFP–neuroligin-2 (CFP-Nlg2) and either HA-MDGA1 or control HA-CD4. Surface trafficking of CFP-Nlg2 was visualized by incubating intact cells with anti-GFP antibodies (which recognize CFP). Ratio of surface to total CFP-Nlg2 did not appear affected by MDGA1. (B) Quantitation of surface trafficking of CFP-Nlg2 on COS7 cells coexpressing HA-MDGA1 or HA-CD4, assessed as intensity ratio of surface anti-GFP antibody signal to CFP signal. *t* test, P = 0.63, *n* = 20 cells each. (C) HEK293T cells were transfected to express the indicated constructs and surface proteins were biotinylated and isolated. Immunoblotting of surface-biotinylated proteins in comparison with whole-cell lysates revealed equivalent surface trafficking of HA–neuroligin-2 (HA-Nlg2) in the presence of YFP-tagged MDGA1 or CD4. (D) Quantitation of the ratio of surface-biotinylated to total HA-Nlg2 in cells coexpressing YFP-MDGA1 or YFP-CD4. *t* test, P = 0.92, *n* = 4. Data are mean ± SEM. Bar, 10 µm.

synapse density assessed by vesicular GABA transporter VGAT, gephyrin, and VGAT-positive gephyrin clusters compared with neighbor nontransfected neurons (Fig. 8, C–E). There was no significant difference in inhibitory synapse markers when the ΔIg1-3 MDGA1 construct was overexpressed, suggesting that binding to neuroligin is needed to mediate the decrease in inhibitory synapses. Furthermore, coexpression of neuroligin-2–CFP significantly rescued VGAT clustering, but not gephyrin clustering, in neurons expressing HA-MDGA1 (Fig. S3). The partial nature of the rescue in this dual overexpression experiment may be due to an elevated ratio of neuroligin-2 to gephyrin, neurexins, and other native synaptic partners, which may disrupt postsynaptic assembly by altering the necessary stoichiometry of interactions. We also examined the number of excitatory synapses assessed by vesicular glutamate transporter VGlut1-positive PSD-95 clusters, but found no significant difference when overexpressing either wild-type or ΔIg1-3 HA-MDGA1 compared with nontransfected neighbors (Fig. 8, A, B, and F). Overexpression of MDGA1 also had no effect on dendritic arborization (Fig. S4). Thus, MDGA1 overexpressed in cultured hippocampal neurons reduces inhibitory but not excitatory synapse density.

Knockdown of MDGA1 increases inhibitory synapse density

Based on the above results, we hypothesized that endogenous MDGA1 may bind neurolign-2 on dendrites, blocking neuroligin-2 interaction with neurexin and limiting inhibitory synapse development. In this case, reducing levels of endogenous MDGA1 in cultured hippocampal neurons should result in increased inhibitory synapse development. To test this hypothesis, we designed a short-hairpin RNA (shRNA) construct to knock down MDGA1. Efficacy and specificity of sh-MDGA1 to knock down HA-MDGA1 but not HA-MDGA2 or an RNAi-resistant HA-MDGA1* with silent mutations was shown in Western blots with cotransfected HEK cells and cultured cortical neurons (Fig. 9 A). Knockdown of MDGA1 in cultured hippocampal neurons significantly increased the number of inhibitory synapses assessed by VGAT-positive gephyrin clusters compared with a control shRNA (sh-con; Fig. 9, B and D). A greater effect was observed on VGAT than on gephyrin (Fig. 9, E and F). The increase in clustering of inhibitory synaptic markers by MDGA1 knockdown was rescued back to control level by coexpression of HA-MDGA1*. In this rescue experiment, HA-MDGA1* was expressed at a low level that had

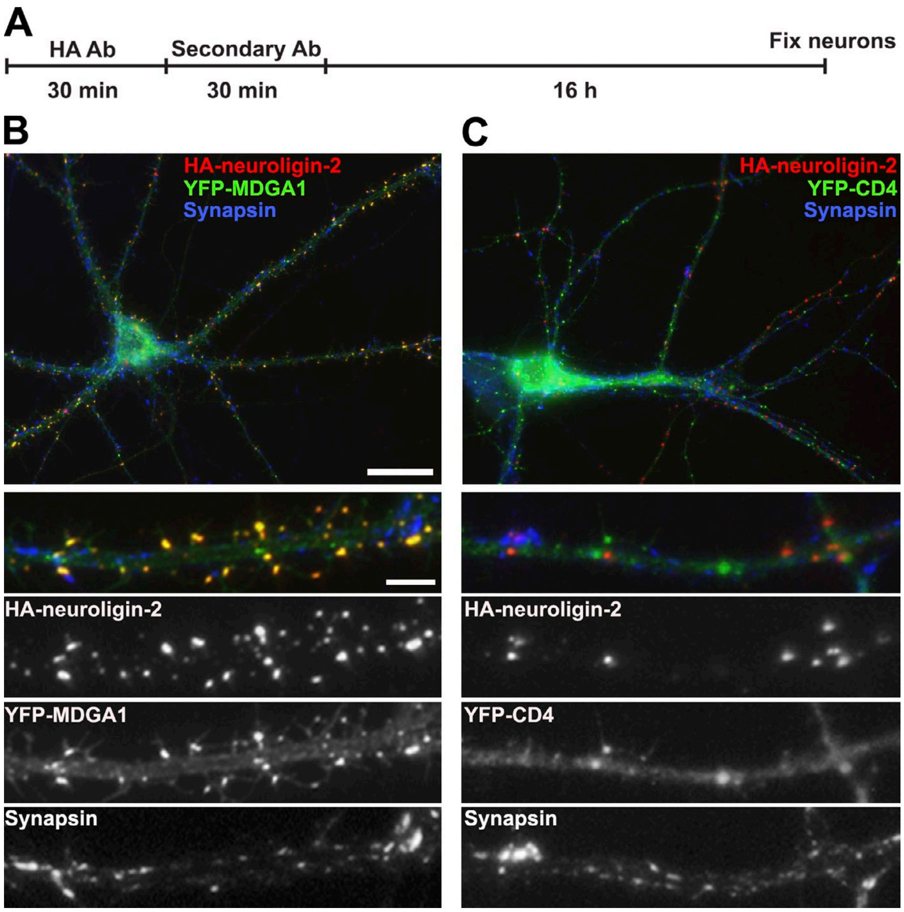

Figure 7. **MDGA1 and neuroligin-2 can interact in cis on dendrites.** Cultured hippocampal neurons were transfected with HA–neuroligin-2 and YFP-MDGA1 or YFP-CD4 control. (A) Live neurons were incubated with rat anti-HA antibody and then Alexa 568–conjugated goat anti–rat antibody to induce surface patching of HA–neuroligin-2, incubated another 16 h, fixed, and imaged. YFP-MDGA1 (B) but not control protein YFP-CD4 (C) co-aggregated with HA–neuroligin-2 at nonsynaptic clusters (lacking apposed synapsin). Bars: (whole cell) 20 µm; (enlarged dendrite regions) 5 µm.

no effect on inhibitory synapse density in control cells (VGAT-positive gephyrin cluster density was 0.189 ± 0.014 per µm in cells expressing sh-con alone and 0.182 ± 0.016 per µm in cells expressing sh-con plus HA-MDGA1*; *t* test, P = 0.789, *n* = 30 cells). Knockdown of MDGA1 had no effect on the number of excitatory synapses assessed by VGlut1-positive PSD-95 clusters (Fig. 9, C and G). Knockdown of MDGA1 also had no effect on dendritic arborization (Fig. S5). These data suggest that endogenous MDGA1 functions to keep inhibitory synapses in check, maintaining inhibitory synapse density at submaximal level.

Discussion

We report here physical and functional interaction between the products of two gene families independently implicated in ASDs and schizophrenia, *MDGA*s and *NLGN*s. Two major findings of this study are: (1) identification of MDGA1 as a negative regulator of inhibitory synapse development, and (2) placement of MDGAs in the neurexin–neuroligin synaptic pathway in which rare mutations contribute to neurodevelopmental disorders. A model of how MDGA1 may suppress inhibitory synapse development is presented in Fig. 10.

Based on these results, MDGA1 is one of very few identified negative regulators of synapse development, in contrast to numerous well-studied positive regulators. Other locally acting negative regulators have been best characterized in *C. elegans*. For example, a Wnt–Frizzled pathway in motor neurons restricts the sites of neuromuscular synapse development (Klassen and Shen, 2007), and the coiled-coil domain protein regulator of synaptogenesis-1, RSY-1, binds and inhibits SYD-2/liprin-α from promoting presynaptic assembly (Patel and Shen, 2009). In mammalian neurons, the transcription factor MEF2, the guanine nucleotide exchange factor Ephexin5, and the cell surface Nogo receptors act through signaling pathways in the postsynaptic cell to negatively regulate the number of excitatory synapses (Flavell et al., 2006; Margolis et al., 2010; Wills et al., 2012). MDGA1 appears distinct in that it selectively suppresses the number of inhibitory synapses and it acts locally in dendrites by directly binding and inhibiting function of the synaptogenic protein neuroligin-2.

Mechanistically, MDGA1 coexpressed with neuroligin-2 inhibited binding of neurexin ectodomain to the neuroligin (Fig. 5, A–D). MDGA1 did not alter the cell surface trafficking of neuroligin-2 (Fig. 6), but did reduce total and surface levels of neuroligin-2 (Figs. 3 and 5). MDGA1 may act in part by reducing neuroligin-2 levels. Yet, when cells with similar levels of neuroligin-2 were compared, robust suppression of synaptogenic activity and neurexin binding were still observed (Figs. 3, 5, and S1). Furthermore, in a binding assay involving only purified ectodomains, the ectodomain of MDGA1 inhibited interaction of neuroligin-2 and neurexin ectodomains (Fig. 5 E). Thus, the simplest potential mechanism is direct steric hindrance; MDGA1 binding to neuroligin-2 on the cell surface may block the binding site for neurexin. The similar apparent K_d of Nlg2-Fc

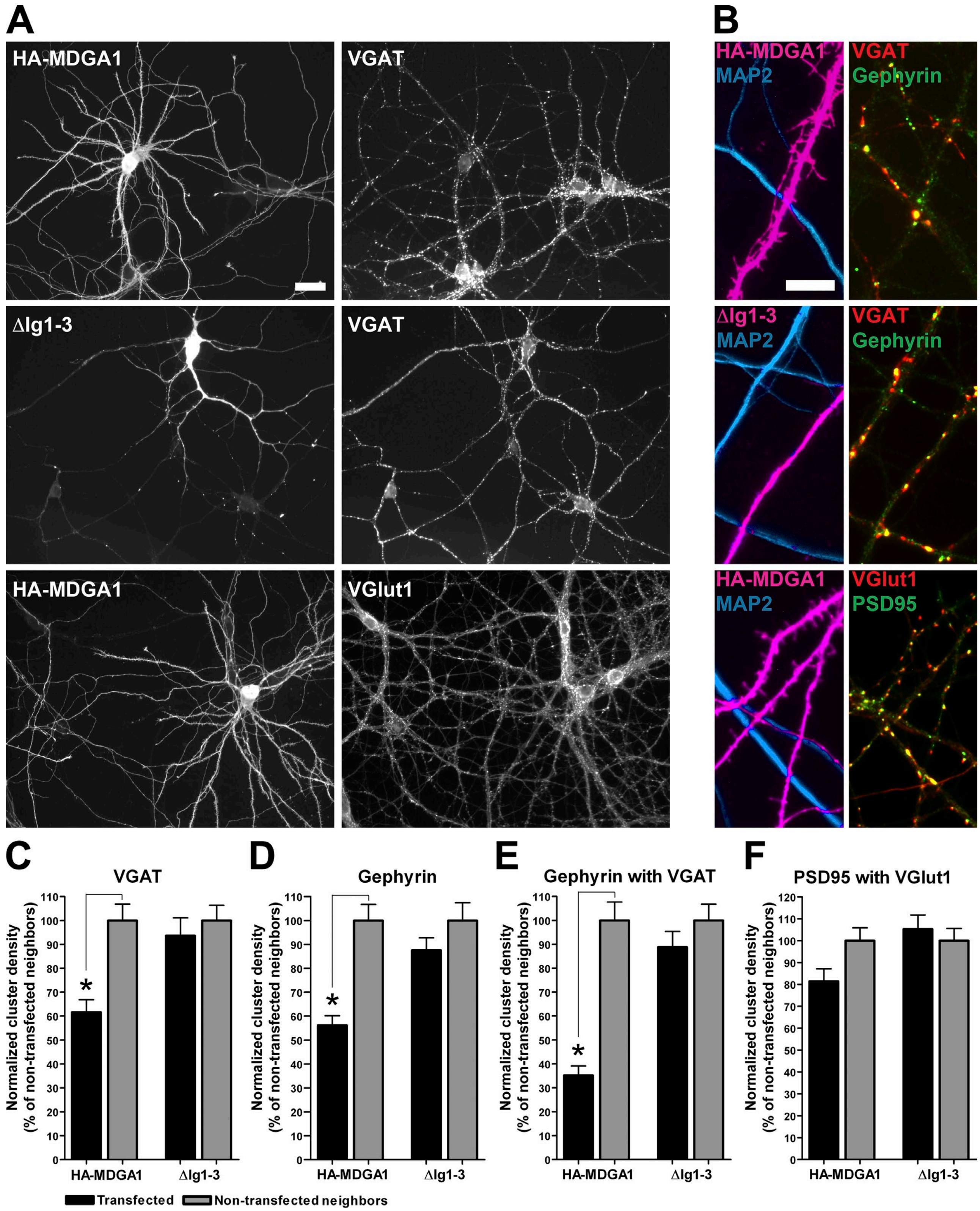

Figure 8. **MDGA1 overexpression reduces inhibitory synapse density.** Cultured hippocampal neurons were transfected at 8–9 DIV with HA-MDGA1 or ΔIg1-3 as a negative control, and then immunostained for indicated synaptic markers and HA tag at 14 DIV. (A) Neurons expressing HA-MDGA1 (top) showed an apparent reduction in inputs with inhibitory presynaptic marker VGAT compared with neighboring untransfected neurons or neurons expressing ΔIg1-3 (middle). Neurons expressing HA-MDGA1 appeared to have normal inputs with excitatory presynaptic marker VGlut1 (bottom). (B) Clusters of VGAT and gephyrin were hardly detected along dendrites expressing HA-MDGA1 (pink, top), whereas such clusters were more readily detected along nontransfected neighboring dendrites (blue, top) or dendrites expressing ΔIg1-3 (pink, middle). Clusters of VGlut1 and PSD-95 along dendrites expressing HA-MDGA1 (pink, bottom) appeared comparable to those along nontransfected neighboring dendrites (blue, bottom). (C–F) Quantitation of number of clusters per dendrite length for VGAT (C), gephyrin (D), VGAT-positive gephyrin (marking inhibitory synapses, E), and VGlut1-positive PSD95 (marking

for cell-expressed MDGA1 and neurexin-1β (7.3 ± 1.0 nM and 8.4 ± 1.1 nM, respectively; Fig. 1) and potent inhibition of neuroligin-2 synaptogenic activity in co-culture (Fig. 3) suggest that MDGA1 may be a powerful inhibitor of neuroligin-2–neurexin interaction and function. Interestingly, only the first three Ig domains plus the GPI membrane anchor of MDGA1 were sufficient to bind Nlg2-Fc and to inhibit neuroligin-2 synaptogenic activity, and all three Ig domains were necessary (Figs. 2 and 4). It is possible that other domains of MDGA may interact with other partners, and indeed the MAM domain can interact with axon-rich brain regions (Fujimura et al., 2006).

MDGA1 and neuroligin-2 can interact in cis on dendrites (Fig. 7), and both overexpression and knockdown studies in cultured hippocampal neurons (Figs. 8 and 9) suggest that a major function of MDGA1 is to suppress inhibitory synapse development in dendrites. Although neurexins, the previously identified extracellular binding partner of neuroligins, are also suggested to function as negative regulators in dendrites (Taniguchi et al., 2007), their major function is in axons to promote synapse development (Dean et al., 2003; Missler et al., 2003; Siddiqui and Craig, 2011; Krueger et al., 2012). Considering the presence of recombinant MDGA1 on the axon surface (Fig. S2 A), the possibility remains open that MDGAs may also function in axons to promote synapse development. It will be important to test MDGA1 and MDGA2 localization and function in multiple circuits in vivo.

The role of MDGA1 to suppress inhibitory synapse development may be explained by its high affinity binding to neuroligin-2 and interference of neuroligin-2 interaction with neurexin. The increase in VGAT clustering with knockdown of MDGA1 (Fig. 9) is similar to effects of overexpressing neuroligin-2 (Chih et al., 2005; Levinson et al., 2005). In contrast, we could not observe high affinity interaction of MDGA1 with neuroligin-1 (Fig. 1), consistent with the lack of any major effect of MDGA1 overexpression or knockdown on excitatory synapses (Figs. 8 and 9). However, the partial localization of recombinant MDGA1 to excitatory postsynaptic sites (Fig. S2) and trend toward reduced excitatory synapses with overexpression of MDGA1 (Fig. 8) leave open the possibility that MDGA1 may have a function at excitatory synapses under some conditions. MDGA1 may interact weakly with neuroligin-1 and/or with neuroligin-3 or neuroligin-4, whose roles are not so well understood. Neuroligin-3 forms complexes in brain with neuroligin-1 and with neuroligin-2 and was localized to both excitatory and inhibitory synapses (Budreck and Scheiffele, 2007). Neuroligin-4 was mainly found at inhibitory glycinergic synapses in retina, brainstem, and spinal cord, but not at GABAergic synapses in brain (Hoon et al., 2011). However, all neuroligins have the capacity to interact with the excitatory postsynaptic scaffold PSD-95 (Irie et al., 1997) and the inhibitory postsynaptic scaffold gephyrin (Poulopoulos et al., 2009), and altering ratios of PSD-95 to neuroligins can alter the balance between excitatory and inhibitory synapses (Prange et al., 2004). Thus, MDGA1 may have complex effects by inhibiting interaction of neuroligin-2 with neurexin, altering the stoichiometry of interaction among neuroligins, neurexins, and other neurexin partners.

Although it is currently difficult to predict how the intronic single nucleotide polymorphisms in *MDGA1* linked to schizophrenia (Kähler et al., 2008; Li et al., 2011) affect protein expression, the exonic deletions in *MDGA2* associated with ASDs would clearly alter protein structure (Bucan et al., 2009). In four cases, only a very short protein truncated before or in the first Ig domain would be produced and in another four cases, a longer protein truncated before or in the MAM domain would be produced (Bucan et al., 2009). Importantly, all of these deletions would remove the GPI membrane anchor, which we predict would be essential to mediate MDGA interaction with neuroligin on the dendritic membrane.

Loss of one allele of *MDGA* might be mimicked by our MDGA1 knockdown, which here resulted in an increase in inhibitory synapse density. Overexpression of neuroligin-2 in transgenic mice also results in increased inhibitory but not excitatory synapse density in frontal cortex, stereotyped behaviors, and impaired social interactions resembling some aspects of ASDs (Hines et al., 2008). Another mouse model of autism, neuroligin-3 R451C knock-in, also exhibits a selective increase in spontaneous inhibitory but not excitatory synaptic transmission in cortex and impaired social interactions (Tabuchi et al., 2007). Exonic deletions or deleterious point mutations in genes encoding excitatory postsynaptic scaffold proteins and dendritic spine signaling components are also implicated in ASDs, and cell culture and animal models exhibit decreases in aspects of glutamatergic synaptic signaling (Penzes et al., 2011; Peça and Feng, 2012). However, not all genetic studies or animal models of nonsyndromic autism support a simple mechanism of increased inhibition or reduced excitation. There is a high incidence of epilepsy with ASDs (Rubenstein and Merzenich, 2003), and even the neuroligin-3 R451C knock-in mice that exhibit increased inhibitory transmission in cortex exhibit increased excitatory transmission in hippocampus (Etherton et al., 2011). It may be that, as in mutations contributing to syndromic autism by altering metabotropic glutamate receptor-mediated protein synthesis (Auerbach et al., 2011), deviations in either direction from the optimal range of inhibition and excitation may contribute to ASDs.

The discovery here that MDGAs interact directly with neuroligins and thus form part of the neurexin–neuroligin synaptic pathway implicated in autism and other neurodevelopmental disorders may help us to better understand the basis of these disorders. The unique function of MDGA1 as a local suppressor of inhibitory synapse development might be exploited toward alleviating multiple disorders involving reduced or enhanced synaptic inhibition.

excitatory synapses, F) in neurons overexpressing HA-MDGA1 or negative control ΔIg1-3. Data are normalized by the value for nontransfected neighboring neurons (gray). ANOVA, $P < 0.0001$ for C–E and $P = 0.03$ for F; $n = 30$ cells each; *, $P < 0.001$ in post-hoc Bonferroni test ($P > 0.05$ in post-hoc Bonferroni test for PSD-95 with VGlut1 for HA-MDGA1 compared with nontransfected neighbors). Data are mean ± SEM. Bars: (A) 30 µm; (B) 10 µm.

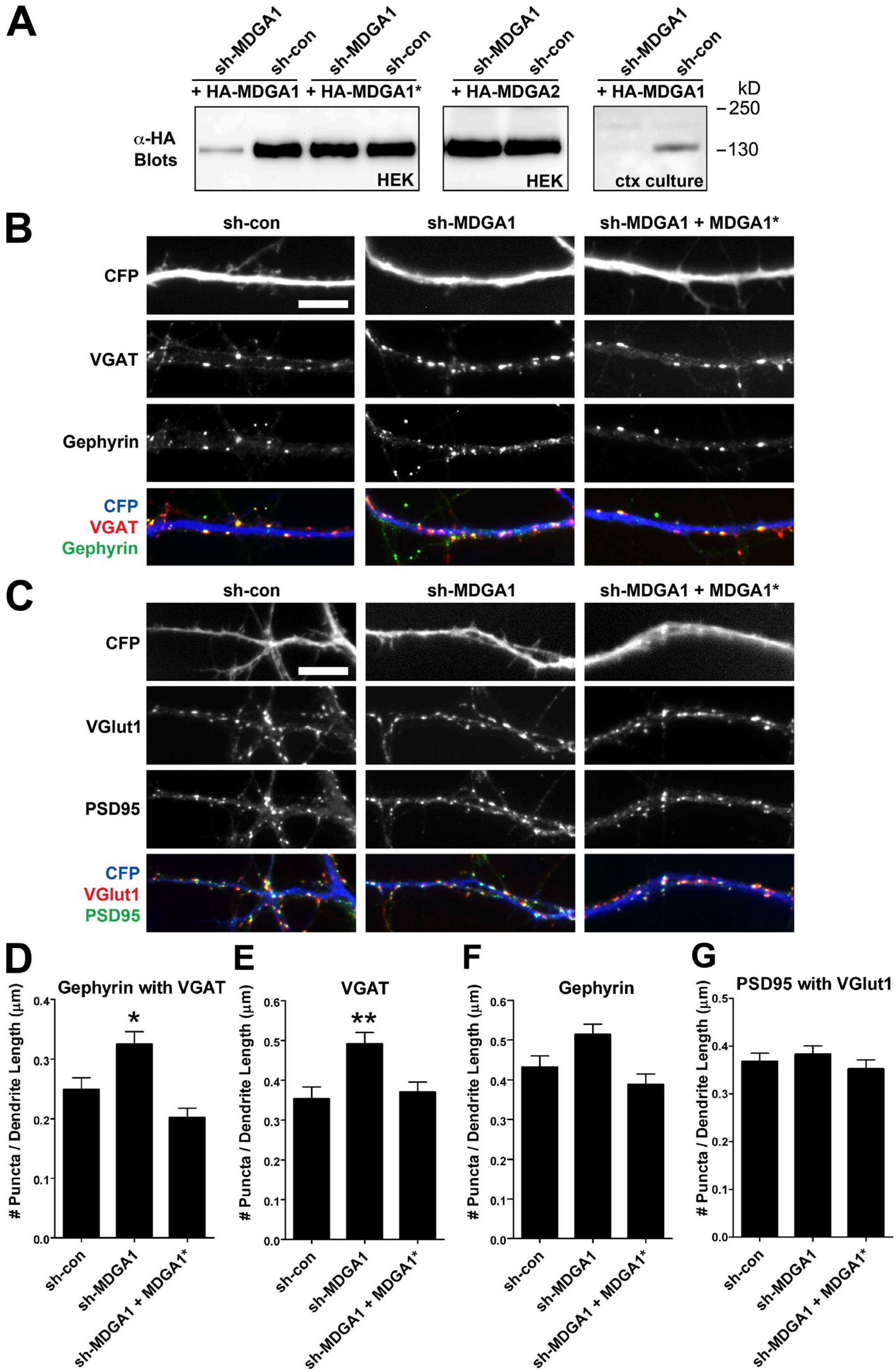
A
sh-MDGA1
sh-con
+ HA-MDGA1
+ HA-MDGA1*
+ HA-MDGA2
kD
250
130
α-HA
Blots
HEK
ctx culture
B
sh-con
sh-MDGA1
sh-MDGA1 + MDGA1*
CFP
VGAT
Gephyrin
C
VGlut1
PSD95
D
Gephyrin with VGAT
E
VGAT
F
Gephyrin
G
PSD95 with VGlut1
Puncta / Dendrite Length (μm)

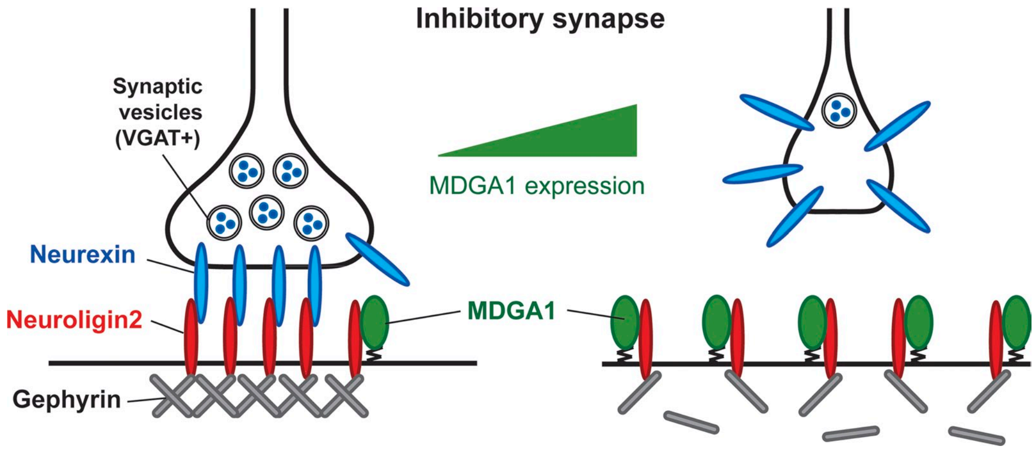

Figure 10. **Model of how MDGA1 may suppress inhibitory synapse development.** Data presented here indicate that MDGA1 binds neuroligin-2 and inhibits its interaction with neurexin, without altering surface trafficking of neuroligin-2. Thus, we propose that high levels of MDGA1 in neurons may suppress inhibitory synapse formation or destabilize inhibitory synapses, resulting in a net reduction in inhibitory synapse density.

Materials and methods

DNA constructs

The cDNA encoding full-length rat MDGA1 was amplified from a rat brain cDNA library (Linhoff et al., 2009). The plasmids for extracellular HA-tagged rat MDGA1 (HA-MDGA1) and HA-tagged mouse MDGA2 (HA-MDGA2) were made by subcloning the mature coding regions of MDGA1 (amino acids [aa] 19–956) and MDGA2 (aa 26–956) into the spHA-C1 vector, a modified EYFP-C1 that expresses HA instead of YFP with an N-terminal signal sequence derived from TrkC cDNA (Takahashi et al., 2011). The plasmid for extracellular YFP-tagged MDGA1 (YFP-MDGA1) was made by subcloning the mature coding region of MDGA1 (aa 19–956) into the spYFP-C1 vector, a modified EYFP-C1 that expresses YFP with an N-terminal signal sequence derived from the NMDA receptor NR2B cDNA (Takahashi et al., 2011). The following HA-MDGA1 deletion constructs were made by inverse PCR: ΔIg1 (aa 24–123 deleted), ΔIg2 (aa 132–230 deleted), ΔIg3 (aa 240–323 deleted), ΔIg1-3 (aa 24–323 deleted), ΔIg4-6 (aa 338–632 deleted), ΔMAM (aa 752–919 deleted), ΔFNIII (aa 641–740 deleted), and Ig1-3 only (aa 338–919 deleted). For overexpression, HA-MDGA1 and Ig1-3 only were subcloned into pCAG-EGFP vector with the CAG promoter. The plasmids for Nlg1-Fc and Nlg2-Fc were made by subcloning the extracellular regions of neuroligin-1 (aa 52–698) and neuroligin-2 (aa 15–676) between the neurexin1β signal sequence and the human IgG Fc cDNA in the vector pc4-sp-Fc modified from pcDNA4 (Takahashi et al., 2011). The plasmid for expressing chicken MDGA1-AP contains the mature coding region of chicken MDGA1 (aa 16–918) in vector APtag5 (Fujimura et al., 2006). For RNA interference knockdown by plasmid-based short-hairpin RNA (sh-RNA), the oligonucleotides that target nucleotides 1027–1045 of rat MDGA1 (5′-GCATCCCTGACAAGTCTAT-3′) were subcloned into LenLox3.7 variant pLL(syn)CFP to express CFP and sh-MDGA1 under the synapsin promoter and U6 promoter, respectively. We used sh-MORB (5′-GATGGTGGCAGTACCAGTG-3′) as a control sh-RNA (sh-con), which has no effects on neuronal morphology, including the densities of excitatory and inhibitory synapses and dendritic spines (Takahashi et al., 2011, 2012). The MDGA1* construct resistant to sh-MDGA1 was generated by the following underlined point mutations: 5′-GCATACCGGATAAAAGTAT-3′. The plasmids encoding HA-CD4 and YFP-CD4 were made by subcloning the mature form of CD4 (aa 27–458) into spHA-C1 and spYFP-C1, respectively. The plasmid for extracellular CFP-tagged neuroligin-1 (CFP-NLG1) was made by replacing HA with CFP in HA-NLG1, a pcDNA3 vector encoding mouse neuroligin-1 with the HA tag between aa 47 and 48 (Graf et al., 2004). The plasmid for extracellular HA-tagged mouse neuroligin-2 (HA-NLG2) contains the signal sequence of mouse neuroligin-1 (aa 1–47) followed by the HA tag and then the mature form of mouse neuroligin-2 (aa 14–836) in pcDNA3. The plasmid for extracellular CFP-tagged neuroligin-2 (CFP-NLG2) was made by replacing HA with CFP in HA-NLG2 (Graf et al., 2004). The plasmid encoding Nrx1β(+S4)-Fc contains the ectodomain of mouse neurexin1β(+S4) (aa 1–292) followed by the human IgG Fc cDNA in pcDNA3 (Graf et al., 2006). The plasmid for HA-neurexin1β(−S4) contains the N-terminal aa 1–262 from mouse neurexin1β fused to the C-terminal sequence for rat neurexin1β and has an HA tag inserted after the signal sequence. All new constructs were verified by DNA sequencing.

Antibodies

The following rabbit polyclonal primary antibodies were used: anti-synapsin (1:2,000, AB1543P; EMD Millipore), anti-VGlut1 (1:2,000, 135 303; Synaptic Systems), anti-VGAT (1:1,000, 131 003; Synaptic Systems), and anti-GFP (1:500, A11122; Invitrogen). The following mouse monoclonal primary antibodies were used: anti-PSD-95 family (1:500, IgG2a, 6G6-1C9; Thermo Fisher Scientific), anti-gephyrin (1:500, IgG1, mAb7a; Synaptic Systems), and anti-HA (1:1,000, IgG2b, 12CA5; Roche). Rat anti-HA (1:1,000, 3F10; Roche) was also used. For labeling dendrites and axons, chicken polyclonal anti-MAP2 (1:4,000, IgY, ab5392; Abcam) and mouse monoclonal anti–Tau-1 (1:2,000, IgG2a, clone PC1C6; EMD Millipore; recognizes dephosphorylated tau) were used, respectively. For secondary antibodies, we used highly cross-adsorbed, Alexa dye–conjugated goat antibodies toward the appropriate species and monoclonal isotype (1:500, Alexa 488, 568, and 647; Invitrogen) and AMCA-conjugated donkey anti–chicken IgY (1:200, 703–155-155; Jackson ImmunoResearch Laboratories, Inc.).

Figure 9. **MDGA1 knockdown increases inhibitory synapse density.** Cultured hippocampal neurons were transfected at 8–9 DIV with a vector coexpressing CFP and a short-hairpin RNA (shRNA) construct corresponding to control shRNA (sh-con) or sh-RNA effective to knock down MDGA1 (sh-MDGA1). Neurons were analyzed at 14 DIV. (A) For shRNA validation, cotransfection of sh-MDGA1 but not sh-con reduced expression of HA-MDGA1 but not the RNAi-resistant form HA-MDGA1* in HEK cells (left gel). Neither sh-con nor sh-MDGA1 reduced expression of HA-MDGA2 in cotransfected HEK cells (middle gel). Knockdown of MDGA1 was also confirmed in cotransfected cortical cultured neurons (ctx culture, right gel). (B and C) In cultured neurons, MDGA1 knockdown appeared to increase the number of VGAT and gephyrin clusters along dendrites (B) but to have no effect on VGlut1 and PSD-95 (C). Co-expression of RNAi-resistant HA-MDGA1* with sh-MDGA1 appeared to normalize clustering of VGAT and gephyrin (B, right column). (D–G) Quantitation of cluster density for VGAT-positive gephyrin marking inhibitory synapses (D), VGAT (E), and gephyrin (F) individually, and VGlut1-positive PSD-95 marking excitatory synapses (G). MDGA1 knockdown selectively increased inhibitory synapse density, with a greater effect on VGAT than on gephyrin. This effect was completely rescued by coexpression of MDGA1*. ANOVA, $P < 0.0001$ for D, $P = 0.0013$ for E, $P = 0.0056$ for F, and $P = 0.48$ for G; $n \geq 40$ cells each; *, $P < 0.05$; **, $P < 0.01$ compared with sh-con in post-hoc Bonferroni test ($P > 0.05$ in post-hoc Bonferroni test for gephyrin for sh-MDGA1 compared with sh-con). Data are mean ± SEM. Bars, 10 µm.

Cell culture, transfection, and immunocytochemistry

Animal care protocols were approved by the University of British Columbia Animal Care Centre. Cultures of hippocampal neurons, COS7 cells, HEK293T cells, neuron-fibroblast co-cultures, transfection, and immunocytochemistry were performed essentially as described previously (Graf et al., 2004, 2006; Takahashi et al., 2012). In brief, hippocampal neurons from E18 rat embryos were cultured at low density on poly-L-lysine–coated glass coverslips inverted over a feeder layer of astrocytes in neurobasal medium (Gibco) supplemented with B27 supplement (Gibco). COS7 and HEK293T cells were cultured in DMEM-H supplemented with 10% fetal bovine serum. For neuron–fibroblast co-culture assays, COS7 cells were transfected using TransIT-LT1 transfection reagent (Mirus) and harvested by trypsinization at 24 h after transfection. Neuron coverslips were flipped into a 12-well plate with conditioned media, and transfected COS7 cells were seeded onto the neuronal growth surface. After 1 h, the coverslips were transferred back into their glial feeder dish. After 1 d of co-culture, the cells were fixed for immunostaining. We used the ProFection Mammalian Transfection System (Promega) for most neuronal transfections, but used the AMAXA nucleofector system (Lonza) for sh-RNA validation in cortical neurons. For immunocytochemistry, cells were fixed with parafix solution (4% paraformaldehyde and 4% sucrose in PBS, pH 7.4) for 15 min followed by permeabilization with 0.25% Triton X-100 in PBS (PBST) or in −20°C methanol for 10 min. For labeling the extracellular-tagged proteins on the cell surface, live cells were incubated with the appropriate antibody against the tag in extracellular solution (ECS: 168 mM NaCl, 2.6 mM KCl, 10 mM Hepes, pH 7.2, 2 mM $CaCl_2$, 2 mM $MgCl_2$, and 10 mM D-glucose) with 100 µg/ml BSA (ECS/BSA) for 30 min at 20°C, and then fixed with parafix solution followed by permeabilization with PBST for immunostaining. To induce surface aggregates of HA–neuroligin-2, live neurons were incubated with anti-HA antibody in the conditioned medium for 30 min followed by the secondary antibody for 30 min. Neurons were returned to the home dish and then fixed 16 h later.

Surface biotinylation and Western blots

Transfected HEK293T cells were washed three times with ice-cold ECS and then incubated with 1 mg/ml EZ-link Sulfo-NHS-LC-Biotin (Thermo Fisher Scientific) in ECS at 4°C for 30 min. The remaining active biotin was quenched by washing three times with ice-cold ECS containing 100 mM glycine. After homogenization in lysate buffer (50 mM Tris–HCl, pH 7.4, 1% Triton X-100, 150 mM NaCl, 1 mM EDTA, 0.5% deoxycholic acid sodium, and a cocktail of protease inhibitors [Roche]), the biotinylated proteins were isolated using streptavidin-conjugated Sepharose beads (Sigma-Aldrich), resolved by SDS-PAGE, and immunoblotted with the corresponding antibodies. For Western blots for shRNA validation, cell lysate was collected, protein concentration was measured with the DC Protein Assay kit (Bio-Rad Laboratories), and equal total protein was loaded per lane for SDS-PAGE and immunoblot with anti-HA antibody.

Production of Fc and AP fusion proteins and binding assays

Nlg2-Fc proteins were produced by HEK293T cells stably expressing the construct (sp4-Nlg2-Fc) through Zeocin-based selection, as described previously (Takahashi et al., 2011). Nlg1-Fc, neurexin1β(+S4)-Fc, MDGA1-AP, neurexin1β-AP, and AP control were produced by HEK293T cells with transient plasmid transfection. The Fc fusion and AP fusion proteins in the conditioned medium were purified using protein G–Sepharose (GE Healthcare) and Ni-NTA Agarose (QIAGEN), respectively. The Fc fusion protein concentration was measured by Western blot relative to a human IgG standard curve. AP fusion protein concentration was measured by Sypro Ruby protein gel staining (Sigma-Aldrich) relative to a BSA standard curve. For the binding assay, transfected live cells were washed with ECS/BSA, and then incubated with purified Fc fusion proteins for 1 h at 20°C followed by incubation with anti-HA antibodies for 30 min. These cells were fixed with parafix solution and then immunostained with FITC-conjugated donkey anti–human IgG (H+L) (1:100; Jackson ImmunoResearch Laboratories, Inc.) and Alexa 568 anti-IgG2b (1:1,000; Invitrogen) to visualize bound Fc fusion proteins and surface HA, respectively.

For the plate-binding assay, 10 µg/ml purified neurexin1β-AP was coated onto the wells of a 96-well MaxiSorp assay plate (Thermo Fisher Scientific) at 4°C overnight. Unbound protein was removed by washing (0.05% Tween 20 in PBS), and remaining surfaces were blocked with blocking buffer (3% BSA and 5% goat serum in PBS) at 37°C for 2 h. 16.6 nM purified Nlg2-Fc was preincubated with 150 nM MDGA1-AP or 150 nM AP control at 37°C for 1 h, and then added to the wells and incubated at 37°C for 2 h. After washing to remove unbound proteins, bound Nlg2-Fc was detected by ELISA with a primary antibody against Fc, a HRP-conjugated second antibody, and TMB substrate (Thermo Fisher Scientific) development to quantify bound Nlg2-Fc by absorbance at 450 nm.

Imaging

Images were acquired on a microscope (Axioplan2; Carl Zeiss) with an oil immersion objective lens (40× 1.30 NA, 63× 1.4 NA, or 25× 0.8 NA) and a cooled CCD camera (Sensys; Photometrics) using MetaMorph imaging software (Molecular Devices) and customized filter sets. Images were acquired as 12-bit grayscale and prepared for presentation using Adobe Photoshop. For quantification, sets of cells were fixed and stained simultaneously and imaged with identical settings. All image acquisition, analysis, and quantification were performed by investigators blind to the experimental condition.

Image analysis and statistical analysis

For quantifying the binding affinity or the surface expression level relative to total, we measured the average intensity of each channel within the delineated COS7 cell area subtracted by the average intensity of off-cell background.

For the co-culture assay, we either measured integrated intensity of synapsin clusters on COS7 cells, or scored the percentage of COS7 cells positive for synapsin clustering, as indicated in the figure legends. We chose COS7 cells coexpressing all transfected constructs from a neurite-rich area. For intensity measurement, synapsin images were thresholded to extract synapsin clusters. The total integrated intensity of all synapsin clusters in the MAP2-negative COS7 cell area was normalized by the total COS7 area from the HA channel. For scoring, COS7 cells were judged as positive or negative for apparent synapsin clustering on the MAP2-negative cell area through direct microscopic observation.

For analysis in overexpression and knockdown experiments, transfected neurons were chosen randomly based on healthy morphology and expression level. Neighboring neurons were chosen based on similar MAP2 staining. Images for each synaptic marker were thresholded to extract the clusters. A dendritic segment per transfected or nontransfected neuron was randomly selected, and the number of clusters per dendrite length was measured. VGLUT1-positive PSD-95 clusters indicate the number of clusters with pixel overlap between the separately thresholded VGLUT1 and PSD-95 channels (and similarly for VGAT-positive gephyrin clusters).

For analysis of dendritic arborization, Sholl analyses were performed with the Sholl Analysis plugin for ImageJ (Anirvan Ghosh Laboratory, University of California, San Diego, La Jolla, CA).

Analysis was performed using MetaMorph 6.1, ImageJ, Excel 2003 (Microsoft), and Prism 4 (GraphPad Software). Statistical comparisons were made with Student's unpaired *t* test or one-way ANOVA with post hoc Bonferroni's multiple comparison test, as indicated in the figure legends. All data are reported as the mean ± SEM from at least two (mostly three) independent experiments.

Online supplemental material

Fig. S1 shows images and quantitative analysis indicating that MDGA1 coexpression with neuroligin-2 in COS7 cell reduces VGAT clustering in contacting axons in co-culture. Fig. S2 shows a diffuse distribution of YFP-MDGA1 along the surface of dendrites and axons of cultured neurons and partial clustering at inhibitory and excitatory postsynaptic sites. Fig. S3 shows that overexpression of neuroligin-2 along with MDGA1 significantly counteracts the effect of MDGA1 on density of VGAT clusters but not of gephyrin clusters. Fig. S4 shows that MDGA1 overexpression does not affect dendritic arborization assessed by Sholl analysis. Fig. S5 shows that MDGA1 knockdown does not affect dendritic arborization assessed by Sholl analysis. Online supplemental material is available at http://www.jcb.org/cgi/content/full/jcb.201206028/DC1.

We thank X. Zhou for excellent preparation of neuron cultures and P. Arstikaitis for helpful discussion.

This work was supported by the NeuroDevNet Canadian Network of Centre of Excellence, National Institutes of Health grant MH070860, and Canada Research Chair awards to A.M. Craig; a Natural Sciences and Engineering Research Council of Canada Postgraduate Scholarship to K.L. Pettem; and a National Alliance for Research on Schizophrenia and Depression (Brain and Behavior Research Fund) Young Investigator grant to H. Takahashi.

Submitted: 7 June 2012
Accepted: 28 December 2012

References

Auerbach, B.D., E.K. Osterweil, and M.F. Bear. 2011. Mutations causing syndromic autism define an axis of synaptic pathophysiology. *Nature*. 480:63–68. http://dx.doi.org/10.1038/nature10658

Betancur, C., T. Sakurai, and J.D. Buxbaum. 2009. The emerging role of synaptic cell-adhesion pathways in the pathogenesis of autism spectrum disorders. *Trends Neurosci.* 32:402–412. http://dx.doi.org/10.1016/j.tins.2009.04.003

Biederer, T., Y. Sara, M. Mozhayeva, D. Atasoy, X. Liu, E.T. Kavalali, and T.C. Südhof. 2002. SynCAM, a synaptic adhesion molecule that drives synapse assembly. *Science*. 297:1525–1531. http://dx.doi.org/10.1126/science.1072356

Boucard, A.A., A.A. Chubykin, D. Comoletti, P. Taylor, and T.C. Südhof. 2005. A splice code for trans-synaptic cell adhesion mediated by binding of neuroligin 1 to alpha- and beta-neurexins. *Neuron*. 48:229–236. http://dx.doi.org/10.1016/j.neuron.2005.08.026

Bourgeron, T. 2009. A synaptic trek to autism. *Curr. Opin. Neurobiol.* 19:231–234. http://dx.doi.org/10.1016/j.conb.2009.06.003

Bucan, M., B.S. Abrahams, K. Wang, J.T. Glessner, E.I. Herman, L.I. Sonnenblick, A.I. Alvarez Retuerto, M. Imielinski, D. Hadley, J.P. Bradfield, et al. 2009. Genome-wide analyses of exonic copy number variants in a family-based study point to novel autism susceptibility genes. *PLoS Genet.* 5:e1000536. http://dx.doi.org/10.1371/journal.pgen.1000536

Budreck, E.C., and P. Scheiffele. 2007. Neuroligin-3 is a neuronal adhesion protein at GABAergic and glutamatergic synapses. *Eur. J. Neurosci.* 26:1738–1748. http://dx.doi.org/10.1111/j.1460-9568.2007.05842.x

Chih, B., H. Engelman, and P. Scheiffele. 2005. Control of excitatory and inhibitory synapse formation by neuroligins. *Science*. 307:1324–1328. http://dx.doi.org/10.1126/science.1107470

Chih, B., L. Gollan, and P. Scheiffele. 2006. Alternative splicing controls selective trans-synaptic interactions of the neuroligin-neurexin complex. *Neuron*. 51:171–178. http://dx.doi.org/10.1016/j.neuron.2006.06.005

Chubykin, A.A., D. Atasoy, M.R. Etherton, N. Brose, E.T. Kavalali, J.R. Gibson, and T.C. Südhof. 2007. Activity-dependent validation of excitatory versus inhibitory synapses by neuroligin-1 versus neuroligin-2. *Neuron*. 54:919–931. http://dx.doi.org/10.1016/j.neuron.2007.05.029

Craig, A.M., E.R. Graf, and M.W. Linhoff. 2006. How to build a central synapse: clues from cell culture. *Trends Neurosci.* 29:8–20. http://dx.doi.org/10.1016/j.tins.2005.11.002

de Bruijn, D.R., A.H. van Dijk, R. Pfundt, A. Hoischen, G.F. Merkx, G.A. Gradek, H. Lybæk, A. Stray-Pedersen, H.G. Brunner, and G. Houge. 2010. Severe progressive autism associated with two de novo changes: A 2.6-Mb 2q31.1 deletion and a balanced t(14;21)(q21.1;p11.2) translocation with long-range epigenetic silencing of LRFN5 expression. *Mol Syndromol*. 1:46–57. http://dx.doi.org/10.1159/000280290

Dean, C., F.G. Scholl, J. Choih, S. DeMaria, J. Berger, E. Isacoff, and P. Scheiffele. 2003. Neurexin mediates the assembly of presynaptic terminals. *Nat. Neurosci.* 6:708–716. http://dx.doi.org/10.1038/nn1074

Etherton, M., C. Földy, M. Sharma, K. Tabuchi, X. Liu, M. Shamloo, R.C. Malenka, and T.C. Südhof. 2011. Autism-linked neuroligin-3 R451C mutation differentially alters hippocampal and cortical synaptic function. *Proc. Natl. Acad. Sci. USA*. 108:13764–13769. http://dx.doi.org/10.1073/pnas.1111093108

Flavell, S.W., C.W. Cowan, T.K. Kim, P.L. Greer, Y. Lin, S. Paradis, E.C. Griffith, L.S. Hu, C. Chen, and M.E. Greenberg. 2006. Activity-dependent regulation of MEF2 transcription factors suppresses excitatory synapse number. *Science*. 311:1008–1012. http://dx.doi.org/10.1126/science.1122511

Fujimura, Y., M. Iwashita, F. Matsuzaki, and T. Yamamoto. 2006. MDGA1, an IgSF molecule containing a MAM domain, heterophilically associates with axon- and muscle-associated binding partners through distinct structural domains. *Brain Res.* 1101:12–19. http://dx.doi.org/10.1016/j.brainres.2006.05.030

Gauthier, J., T.J. Siddiqui, P. Huashan, D. Yokomaku, F.F. Hamdan, N. Champagne, M. Lapointe, D. Spiegelman, A. Noreau, R.G. Lafrenière, et al. 2011. Truncating mutations in NRXN2 and NRXN1 in autism spectrum disorders and schizophrenia. *Hum. Genet.* 130:563–573. http://dx.doi.org/10.1007/s00439-011-0975-z

Gibson, J.R., K.M. Huber, and T.C. Südhof. 2009. Neuroligin-2 deletion selectively decreases inhibitory synaptic transmission originating from fast-spiking but not from somatostatin-positive interneurons. *J. Neurosci.* 29:13883–13897. http://dx.doi.org/10.1523/JNEUROSCI.2457-09.2009

Glessner, J.T., K. Wang, G. Cai, O. Korvatska, C.E. Kim, S. Wood, H. Zhang, A. Estes, C.W. Brune, J.P. Bradfield, et al. 2009. Autism genome-wide copy number variation reveals ubiquitin and neuronal genes. *Nature*. 459:569–573. http://dx.doi.org/10.1038/nature07953

Graf, E.R., X. Zhang, S.X. Jin, M.W. Linhoff, and A.M. Craig. 2004. Neurexins induce differentiation of GABA and glutamate postsynaptic specializations via neuroligins. *Cell*. 119:1013–1026. http://dx.doi.org/10.1016/j.cell.2004.11.035

Graf, E.R., Y. Kang, A.M. Hauner, and A.M. Craig. 2006. Structure function and splice site analysis of the synaptogenic activity of the neurexin-1 beta LNS domain. *J. Neurosci.* 26:4256–4265. http://dx.doi.org/10.1523/JNEUROSCI.1253-05.2006

Hines, R.M., L. Wu, D.J. Hines, H. Steenland, S. Mansour, R. Dahlhaus, R.R. Singaraja, X. Cao, E. Sammler, S.G. Hormuzdi, et al. 2008. Synaptic imbalance, stereotypies, and impaired social interactions in mice with altered neuroligin 2 expression. *J. Neurosci.* 28:6055–6067. http://dx.doi.org/10.1523/JNEUROSCI.0032-08.2008

Hoon, M., T. Soykan, B. Falkenburger, M. Hammer, A. Patrizi, K.F. Schmidt, M. Sassoè-Pognetto, S. Löwel, T. Moser, H. Taschenberger, et al. 2011. Neuroligin-4 is localized to glycinergic postsynapses and regulates inhibition in the retina. *Proc. Natl. Acad. Sci. USA*. 108:3053–3058. http://dx.doi.org/10.1073/pnas.1006946108

Irie, M., Y. Hata, M. Takeuchi, K. Ichtchenko, A. Toyoda, K. Hirao, Y. Takai, T.W. Rosahl, and T.C. Südhof. 1997. Binding of neuroligins to PSD-95. *Science*. 277:1511–1515. http://dx.doi.org/10.1126/science.277.5331.1511

Ishikawa, T., N. Gotoh, C. Murayama, T. Abe, M. Iwashita, F. Matsuzaki, T. Suzuki, and T. Yamamoto. 2011. IgSF molecule MDGA1 is involved in radial migration and positioning of a subset of cortical upper-layer neurons. *Dev. Dyn.* 240:96–107. http://dx.doi.org/10.1002/dvdy.22496

Jamain, S., K. Radyushkin, K. Hammerschmidt, S. Granon, S. Boretius, F. Varoqueaux, N. Ramanantsoa, J. Gallego, A. Ronnenberg, D. Winter, et al. 2008. Reduced social interaction and ultrasonic communication in a mouse model of monogenic heritable autism. *Proc. Natl. Acad. Sci. USA*. 105:1710–1715. http://dx.doi.org/10.1073/pnas.0711555105

Kähler, A.K., S. Djurovic, B. Kulle, E.G. Jönsson, I. Agartz, H. Hall, S. Opjordsmoen, K.D. Jakobsen, T. Hansen, I. Melle, et al. 2008. Association analysis of schizophrenia on 18 genes involved in neuronal migration: MDGA1 as a new susceptibility gene. *Am. J. Med. Genet. B. Neuropsychiatr. Genet.* 147B:1089–1100. http://dx.doi.org/10.1002/ajmg.b.30726

Klassen, M.P., and K. Shen. 2007. Wnt signaling positions neuromuscular connectivity by inhibiting synapse formation in *C. elegans*. *Cell*. 130:704–716. http://dx.doi.org/10.1016/j.cell.2007.06.046

Krueger, D.D., L.P. Tuffy, T. Papadopoulos, and N. Brose. 2012. The role of neurexins and neuroligins in the formation, maturation, and function of vertebrate synapses. *Curr. Opin. Neurobiol.* 22:412–422. http://dx.doi.org/10.1016/j.conb.2012.02.012

Lein, E.S., M.J. Hawrylycz, N. Ao, M. Ayres, A. Bensinger, A. Bernard, A.F. Boe, M.S. Boguski, K.S. Brockway, E.J. Byrnes, et al. 2007. Genome-wide atlas of gene expression in the adult mouse brain. *Nature*. 445:168–176. http://dx.doi.org/10.1038/nature05453

Levinson, J.N., N. Chéry, K. Huang, T.P. Wong, K. Gerrow, R. Kang, O. Prange, Y.T. Wang, and A. El-Husseini. 2005. Neuroligins mediate excitatory and inhibitory synapse formation: involvement of PSD-95 and neurexin-1beta in neuroligin-induced synaptic specificity. *J. Biol. Chem.* 280:17312–17319. http://dx.doi.org/10.1074/jbc.M413812200

Li, J., J. Liu, G. Feng, T. Li, Q. Zhao, Y. Li, Z. Hu, L. Zheng, Z. Zeng, L. He, et al. 2011. The MDGA1 gene confers risk to schizophrenia and bipolar disorder. *Schizophr. Res.* 125:194–200. http://dx.doi.org/10.1016/j.schres.2010.11.002

Linhoff, M.W., J. Laurén, R.M. Cassidy, F.A. Dobie, H. Takahashi, H.B. Nygaard, M.S. Airaksinen, S.M. Strittmatter, and A.M. Craig. 2009. An unbiased expression screen for synaptogenic proteins identifies the LRRTM protein family as synaptic organizers. *Neuron*. 61:734–749. http://dx.doi.org/10.1016/j.neuron.2009.01.017

Litwack, E.D., R. Babey, R. Buser, M. Gesemann, and D.D. O'Leary. 2004. Identification and characterization of two novel brain-derived immunoglobulin superfamily members with a unique structural organization. *Mol. Cell. Neurosci.* 25:263–274. http://dx.doi.org/10.1016/j.mcn.2003.10.016

Mah, W., J. Ko, J. Nam, K. Han, W.S. Chung, and E. Kim. 2010. Selected SALM (synaptic adhesion-like molecule) family proteins regulate synapse formation. *J. Neurosci.* 30:5559–5568. http://dx.doi.org/10.1523/JNEUROSCI.4839-09.2010

Margolis, S.S., J. Salogiannis, D.M. Lipton, C. Mandel-Brehm, Z.P. Wills, A.R. Mardinly, L. Hu, P.L. Greer, J.B. Bikoff, H.Y. Ho, et al. 2010. EphB-mediated degradation of the RhoA GEF Ephexin5 relieves a developmental brake on excitatory synapse formation. *Cell*. 143:442–455. http://dx.doi.org/10.1016/j.cell.2010.09.038

Missler, M., W. Zhang, A. Rohlmann, G. Kattenstroth, R.E. Hammer, K. Gottmann, and T.C. Südhof. 2003. Alpha-neurexins couple Ca2+ channels to synaptic vesicle exocytosis. *Nature*. 423:939–948. http://dx.doi.org/10.1038/nature01755

Patel, M.R., and K. Shen. 2009. RSY-1 is a local inhibitor of presynaptic assembly in *C. elegans*. *Science*. 323:1500–1503. http://dx.doi.org/10.1126/science.1169025

Peça, J., and G. Feng. 2012. Cellular and synaptic network defects in autism. *Curr. Opin. Neurobiol.* 22:866–872. http://dx.doi.org/10.1016/j.conb.2012.02.015

Penzes, P., M.E. Cahill, K.A. Jones, J.E. VanLeeuwen, and K.M. Woolfrey. 2011. Dendritic spine pathology in neuropsychiatric disorders. *Nat. Neurosci.* 14:285–293. http://dx.doi.org/10.1038/nn.2741

Pinto, D., A.T. Pagnamenta, L. Klei, R. Anney, D. Merico, R. Regan, J. Conroy, T.R. Magalhaes, C. Correia, B.S. Abrahams, et al. 2010. Functional impact of global rare copy number variation in autism spectrum disorders. *Nature*. 466:368–372. http://dx.doi.org/10.1038/nature09146

Piton, A., J.L. Michaud, H. Peng, S. Aradhya, J. Gauthier, L. Mottron, N. Champagne, R.G. Lafrenière, F.F. Hamdan, R. Joober, et al; S2D team. 2008. Mutations in the calcium-related gene IL1RAPL1 are associated with autism. *Hum. Mol. Genet.* 17:3965–3974. http://dx.doi.org/10.1093/hmg/ddn300

Poulopoulos, A., G. Aramuni, G. Meyer, T. Soykan, M. Hoon, T. Papadopoulos, M. Zhang, I. Paarmann, C. Fuchs, K. Harvey, et al. 2009. Neuroligin 2 drives postsynaptic assembly at perisomatic inhibitory synapses through gephyrin and collybistin. *Neuron*. 63:628–642. http://dx.doi.org/10.1016/j.neuron.2009.08.023

Prange, O., T.P. Wong, K. Gerrow, Y.T. Wang, and A. El-Husseini. 2004. A balance between excitatory and inhibitory synapses is controlled by PSD-95 and neuroligin. *Proc. Natl. Acad. Sci. USA*. 101:13915–13920. http://dx.doi.org/10.1073/pnas.0405939101

Rubenstein, J.L., and M.M. Merzenich. 2003. Model of autism: increased ratio of excitation/inhibition in key neural systems. *Genes Brain Behav.* 2:255–267. http://dx.doi.org/10.1034/j.1601-183X.2003.00037.x

Sanders, S.J., A.G. Ercan-Sencicek, V. Hus, R. Luo, M.T. Murtha, D. Moreno-De-Luca, S.H. Chu, M.P. Moreau, A.R. Gupta, S.A. Thomson, et al. 2011. Multiple recurrent de novo CNVs, including duplications of the 7q11.23 Williams syndrome region, are strongly associated with autism. *Neuron*. 70:863–885. http://dx.doi.org/10.1016/j.neuron.2011.05.002

Scheiffele, P., J. Fan, J. Choih, R. Fetter, and T. Serafini. 2000. Neuroligin expressed in nonneuronal cells triggers presynaptic development in contacting axons. *Cell*. 101:657–669. http://dx.doi.org/10.1016/S0092-8674(00)80877-6

Siddiqui, T.J., and A.M. Craig. 2011. Synaptic organizing complexes. *Curr. Opin. Neurobiol.* 21:132–143. http://dx.doi.org/10.1016/j.conb.2010.08.016

Siddiqui, T.J., R. Pancaroglu, Y. Kang, A. Rooyakkers, and A.M. Craig. 2010. LRRTMs and neuroligins bind neurexins with a differential code to cooperate in glutamate synapse development. *J. Neurosci.* 30:7495–7506. http://dx.doi.org/10.1523/JNEUROSCI.0470-10.2010

Soler-Llavina, G.J., M.V. Fuccillo, J. Ko, T.C. Südhof, and R.C. Malenka. 2011. The neurexin ligands, neuroligins and leucine-rich repeat transmembrane proteins, perform convergent and divergent synaptic functions in vivo. *Proc. Natl. Acad. Sci. USA*. 108:16502–16509. http://dx.doi.org/10.1073/pnas.1114028108

Song, J.Y., K. Ichtchenko, T.C. Südhof, and N. Brose. 1999. Neuroligin 1 is a postsynaptic cell-adhesion molecule of excitatory synapses. *Proc. Natl. Acad. Sci. USA*. 96:1100–1105. http://dx.doi.org/10.1073/pnas.96.3.1100

Südhof, T.C. 2008. Neuroligins and neurexins link synaptic function to cognitive disease. *Nature*. 455:903–911. http://dx.doi.org/10.1038/nature07456

Sun, C., M.C. Cheng, R. Qin, D.L. Liao, T.T. Chen, F.J. Koong, G. Chen, and C.H. Chen. 2011. Identification and functional characterization of rare mutations of the neuroligin-2 gene (NLGN2) associated with schizophrenia. *Hum. Mol. Genet.* 20:3042–3051. http://dx.doi.org/10.1093/hmg/ddr208

Szatmari, P., A.D. Paterson, L. Zwaigenbaum, W. Roberts, J. Brian, X.Q. Liu, J.B. Vincent, J.L. Skaug, A.P. Thompson, L. Senman, et al; Autism Genome Project Consortium. 2007. Mapping autism risk loci using genetic linkage and chromosomal rearrangements. *Nat. Genet.* 39:319–328. http://dx.doi.org/10.1038/ng1985

Tabuchi, K., J. Blundell, M.R. Etherton, R.E. Hammer, X. Liu, C.M. Powell, and T.C. Südhof. 2007. A neuroligin-3 mutation implicated in autism increases inhibitory synaptic transmission in mice. *Science*. 318:71–76. http://dx.doi.org/10.1126/science.1146221

Takahashi, H., P. Arstikaitis, T. Prasad, T.E. Bartlett, Y.T. Wang, T.H. Murphy, and A.M. Craig. 2011. Postsynaptic TrkC and presynaptic PTPσ function as a bidirectional excitatory synaptic organizing complex. *Neuron*. 69:287–303. http://dx.doi.org/10.1016/j.neuron.2010.12.024

Takahashi, H., K. Katayama, K. Sohya, H. Miyamoto, T. Prasad, Y. Matsumoto, M. Ota, H. Yasuda, T. Tsumoto, J. Aruga, and A.M. Craig. 2012. Selective control of inhibitory synapse development by Slitrk3-PTPδ trans-synaptic interaction. *Nat. Neurosci.* 15:389–398: S1–S2. http://dx.doi.org/10.1038/nn.3040

Takeuchi, A., and D.D. O'Leary. 2006. Radial migration of superficial layer cortical neurons controlled by novel Ig cell adhesion molecule MDGA1. *J. Neurosci.* 26:4460–4464. http://dx.doi.org/10.1523/JNEUROSCI.4935-05.2006

Taniguchi, H., L. Gollan, F.G. Scholl, V. Mahadomrongkul, E. Dobler, N. Limthong, M. Peck, C. Aoki, and P. Scheiffele. 2007. Silencing of neuroligin function by postsynaptic neurexins. *J. Neurosci.* 27:2815–2824. http://dx.doi.org/10.1523/JNEUROSCI.0032-07.2007

Vaags, A.K., A.C. Lionel, D. Sato, M. Goodenberger, Q.P. Stein, S. Curran, C. Ogilvie, J.W. Ahn, I. Drmic, L. Senman, et al. 2012. Rare deletions at the neurexin 3 locus in autism spectrum disorder. *Am. J. Hum. Genet.* 90:133–141. http://dx.doi.org/10.1016/j.ajhg.2011.11.025

Valnegri, P., C. Montrasio, D. Brambilla, J. Ko, M. Passafaro, and C. Sala. 2011. The X-linked intellectual disability protein IL1RAPL1 regulates excitatory synapse formation by binding PTPδ and RhoGAP2. *Hum. Mol. Genet.* 20:4797–4809. http://dx.doi.org/10.1093/hmg/ddr418

Varoqueaux, F., S. Jamain, and N. Brose. 2004. Neuroligin 2 is exclusively localized to inhibitory synapses. *Eur. J. Cell Biol.* 83:449–456. http://dx.doi.org/10.1078/0171-9335-00410

Varoqueaux, F., G. Aramuni, R.L. Rawson, R. Mohrmann, M. Missler, K. Gottmann, W. Zhang, T.C. Südhof, and N. Brose. 2006. Neuroligins determine synapse maturation and function. *Neuron*. 51:741–754. http://dx.doi.org/10.1016/j.neuron.2006.09.003

Wills, Z.P., C. Mandel-Brehm, A.R. Mardinly, A.E. McCord, R.J. Giger, and M.E. Greenberg. 2012. The nogo receptor family restricts synapse number in the developing hippocampus. *Neuron*. 73:466–481. http://dx.doi.org/10.1016/j.neuron.2011.11.029

Yoshida, T., M. Yasumura, T. Uemura, S.J. Lee, M. Ra, R. Taguchi, Y. Iwakura, and M. Mishina. 2011. IL-1 receptor accessory protein-like 1 associated with mental retardation and autism mediates synapse formation by trans-synaptic interaction with protein tyrosine phosphatase δ. *J. Neurosci.* 31:13485–13499. http://dx.doi.org/10.1523/JNEUROSCI.2136-11.2011

Zhiling, Y., E. Fujita, Y. Tanabe, T. Yamagata, T. Momoi, and M.Y. Momoi. 2008. Mutations in the gene encoding CADM1 are associated with autism spectrum disorder. *Biochem. Biophys. Res. Commun.* 377:926–929. http://dx.doi.org/10.1016/j.bbrc.2008.10.107